Resource Management in Solar Powered Wireless Mesh Networks

RESOURCE MANAGEMENT IN SOLAR POWERED WIRELESS MESH NETWORKS

BY

GHADA BADAWY, M.Sc.

A THESIS

SUBMITTED TO THE DEPARTMENT OF ELECTRICAL & COMPUTER ENGINEERING

AND THE SCHOOL OF GRADUATE STUDIES

OF MCMASTER UNIVERSITY

IN PARTIAL FULFILMENT OF THE REQUIREMENTS

FOR THE DEGREE OF

DOCTOR OF PHILOSOPHY

Doctor of Philosophy (2010) McMaster University

(Electrical & Computer Engineering) Hamilton, Ontario, Canada

TITLE:	Resource Management in Solar Powered Wireless Mesh Networks
AUTHOR:	Ghada Badawy M.Sc., (Computer Engineering) Cairo University, Cairo, Egypt
SUPERVISOR:	Dr. Terence D. Todd
NUMBER OF PAGES:	xv, 80

Abstract

Wireless mesh networks are now being used to deploy radio coverage in a large variety of outdoor applications. One of the major obstacles that these networks face is that of providing the nodes with electrical power and wired network connections. Solar powered mesh nodes are increasingly used to eliminate the need for these types of connections, making the nodes truly tether-less. In these types of networks however, the cost of the energy collection and storage components can be a significant fraction of the total node cost, which motivates a careful selection of these resources.

This thesis focusses on key issues relating to the deployment and operation of solar powered wireless mesh networks. First, the problem of provisioning the mesh nodes with a suitable solar panel and battery configuration is considered. This is done by assuming a bandwidth usage profile and using historical solar insolation data for the desired deployment location. A resource provisioning algorithm is proposed based on the use of temporal shortest-path routing and taking into account the node energy-flow for the target deployment time period. A methodology is introduced which uses a genetic algorithm (GA) to incorporate energy-aware routing into the resource assignment procedure. Results show that the proposed resource provisioning algorithm can achieve large cost savings when compared to conventional provisioning methods.

During post-deployment network operation, the actual bandwidth profile and solar insolation may be different than that for which the nodes were originally provisioned. To prevent node outage, the network must reduce its workload by flow controlling its input traffic. The problem of admitting network bandwidth flows in a fair manner is also studied. A bound is first formulated which achieves the best max/min fair flow control subject to eliminating node outage. The bound motivates a proposed causal flow control algorithm whose operation uses prediction based on access to on-line historical weather data. The results show that the proposed algorithm performs well when compared to the analytic bound that is derived for this problem.

Finally, as user traffic evolves, the network resources need to be updated. This problem is considered using a minimum cost upgrade objective. A mixed integer linear programming (MILP) formulation is derived to obtain a lower bound on the network update cost. A genetic algorithm is used to determine practical cost-effective network resource upgrading. The results show that the proposed methodology can obtain significant cost savings.

Acknowledgements

I would like to express my sincere thanks to my supervisor, Dr. Terence D. Todd for his guidance and support throughout my graduate studies at McMaster University. Working under his supervision has been a great chance for me to learn in both academic and non-academic areas. Indeed, his consistent help and support made it possible for me to finish this work. I am grateful to the members of my Ph.D. supervisory committee and the members of the examining committee for reading my thesis and for their valuable suggestions and comments. Also, I would like to thank all the members of the Wireless Networking Group, for their helpful discussions. I would like to thank my parents for always believing in me and encouraging me throughout the years.

At last but not least, I would like to give special thanks to my husband and my daughter. Their love and support pushed me to be the best I can be, and their patience has made this thesis a dream come true.

Abbreviations

AC	Access Category
AC	Alternating Current
AP	Access Point
APSD	Automatic Power Save Delivery
BSP	Base Station Positioning
BSS	Basic Service Set
BUP	Bandwidth Usage Profile
CR	Competitive Ratio
CAC	Call Admission Control
CAP	Controlled Access Phase
CFP	Contention Free Period
CP	Contention Period
CSMA/CA	Carrier Sense Multiple Access with Collision Avoidance
DCF	Distributed Coordination Function
DS	Distribution System
DIFS	DCF Inter Frame Space
DTIM	Delivery Traffic Indication Message

EDCA	Enhanced Distributed Channel Access
ESS	Extended Service Set
EARP	Energy Aware Resource Provisioning
FFRBC	Fair Fixed Rate Bandwidth Control
FVRBC	Fair Variable Rate Bandwidth Control
GA	Genetic Algorithm
GPS	Global Positioning System
HC	Hybrid Coordinator
HCCA	HCF Controlled Channel Access
HCF	Hybrid Coordination Function
IBSS	Independent Basic Service Set
IEEE	Institute of Electrical and Electronics Engineers
IP	Internet Protocol
LAN	Local Area Network
LP	Linear Programming
MAC	Medium Access Control
MAP	Mesh Access Point
MILP	Mixed Integer Linear Programming
MP	Mesh Point
MS	Mobile Station
MSDU	MAC Service Data Unit
NAM	Network Allocation Map
NAV	Network Allocation Vector

NIC	Network Interface Card
NIST	National Institute of Standards and Technology
NREL	National Renewable Energy Laboratory
NSRDB	National Solar Radiation DataBase
OFDM	Orthogonal Frequency Division Multiplexing
PCF	Point Coordination Function
PHY	Physical Layer
PoE	Power over Ethernet
PS	Power Saving
PV	Photo-Voltaic
PIFS	PCF Inter Frame Space
QoS	Quality of Service
RTS/CTS	Request to Send/ Clear to Send
S-APSD	Scheduled Automatic Power Save Delivery
SMAP	Solar Powered MAP
S-PSMP	Scheduled PSMP
SPRP	Shortest Path Resource Provisioning
STA	Station
SIFS	Short Inter Frame Space
SP	Service Period
TGM	Traffic Growth Management
TGMGA	Traffic Growth Management using GA
TBTT	Target Beacon Transmission Time

TC	Traffic Class
TIM	Traffic Indication Message
TXOP	Transmit Opportunity
U-APSD	Unscheduled APSD
UMTS	Universal Mobile Telecommunication System
U-PSMP	Unscheduled PSMP
VoIP	Voice over IP
WLAN	Wireless Local Area Network
WMN	Wireless Mesh Network

Contents

List of Figures

List of Tables

Chapter 1

Introduction

1.1 Overview

Wireless mesh networks (WMNs) are a promising technology that uses multi-hop radio communications. These types of networks are gaining significant attention as a cost effective way to establish robust and reliable broadband services for end users. Wireless mesh networks consist of mesh clients, mesh routers and gateways. The mesh clients are often laptops, cell phones and other wireless end user devices while the mesh routers forward traffic to and from the gateways which provide a connection to the Internet.

Wireless mesh networks are increasingly used to provide radio coverage in many permanent metropolitan area deployments. In many of these cases, radio coverage is required over expansive outdoor areas. One of the major obstacles that these networks face is that of providing the nodes with electrical power and wired network connections. Although power can sometimes be supplied through power over Ethernet connections, such a solution requires a wired network connection, which may not exist.

An alternative to continuous power connections is to operate some of the mesh nodes using a sustainable energy source such as solar power. These kinds of nodes can be quickly installed and have additional node positioning advantages compared with conventional mesh nodes, since the solar powered nodes are completely tether-less. This thesis considers the design and configuration of these types of networks.

Electrical devices which operate using solar power are referred to as photo-voltaic (PV) systems. An objective in the design of most PV systems is to ensure that the solar panel and battery resources are sufficient to provide an uninterrupted source of power. If at any time a node's battery level drops below a certain energy threshold, the mesh node electronics will experience a power outage. Before a network is installed, the nodes must be provisioned with a solar panel and battery combination that is sufficient to accommodate each node's anticipated workload. The assigned configuration for each node must be such that the network survives without node outage for the desired deployment duration. This assignment

typically uses "geographic provisioning" to account for the solar insolation available at the network's deployment location. Depending on the geographic location of the node and the expected workload, the cost of the batteries and the solar panels can be a significant fraction of the total network cost, which motivates a careful selection of the allocated resources.

1.2 Resource Management in Wireless Mesh Networks

This thesis focusses on the most important issues related to the deployment and operation of solar powered wireless mesh networks. In traditional wireless mesh networks, two of the main design objectives are to minimize cost in the planning phase and to maximize node reliability when the network is in operation. Designing networks that include solar powered nodes is a challenging task when compared to traditional network design. The node costs are highly sensitive to the network's geographic location and the mesh node's workload, meaning that the network designer must take this into account in order to reduce costs.

Solar powered wireless mesh nodes must be provisioned with a solar panel and battery combination that is sufficient to prevent node outage. This is normally done by assuming an energy workload for each node, and then by assigning resources that are based on results obtained using historical meteorological data for the geographic location where the network is to be deployed (Farbod and Todd, 2006). This thesis introduces a methodology for determining the resource assignment based on conventional mechanisms where the individual node bandwidth flows must be determined prior to doing the resource assignment. A methodology that uses genetic algorithms (GA) to incorporate energy-aware routing into the resource assignment procedure is also introduced. A linear programming formulation is developed with the objective of obtaining a minimum total network cost resource assignment, subject to satisfying the target bandwidth flow profile, and accounting for the desired geographic deployment location. Results are presented which show the large resource savings that energy aware resource assignment can achieve when compared to that done using conventional resource assignment.

Operating the deployed network using the minimum provisioning which achieves outage-free operation does not guarantee that the network will be outage-free in the future, since the past data are only random sample functions of the solar insolation process. Also, future aggregate bandwidth demands may exceed the assumed load profile. For this reason, the derived provisionings are usually either increased by some safety factor (i.e., the open loop case), or, the nodes must use some form of closed-loop outage control as discussed in (Sayegh and Todd, 2007). The thesis next considers this bandwidth control problem. Bandwidth control must flow control input traffic in such a way that outage is prevented and yet the best possible performance is obtained. This control action will result in a bandwidth deficit and should be applied in a manner that is both temporally and spatially fair.

The thesis proposes a mechanism for controlling the requested bandwidth in order to guarantee sustainable and yet fair operation. The problem is first formulated as an optimization using a convex utility fairness function. Using this optimization, a non-causal max/min fairness bound is obtained based on knowledge of future solar insolation data and traffic flows. Then a bandwidth control algorithm that is motivated by the optimization framework is presented, which uses solar insolation prediction based on access to on-line historical weather data. The results show that the proposed algorithm eliminates node outage and performs very well compared to the optimum bandwidth control bound for a variety of network scenarios.

Finally, since users have come to expect a ubiquitous presence of wireless services, the traffic volume in a deployed wireless mesh network may grow with time. This will drive the need to periodically upgrade the network to meet these increasing traffic demands. To address this problem, traditional traffic growth management typically includes the process of network capacity upgrading, which may involve adding new nodes and transmission links where they are needed. In the case of solar powered networks, one must also consider the costs of updating the energy source and storage configurations of the nodes in order that the long-term sustainability of the network can be preserved. Traffic growth management deals with the network upgrade problem, where the overall traffic load on the network continues to grow with time. The thesis proposes and studies a methodology for addressing the problem of traffic evolution. A performance bound on the network upgrade cost is formulated as a mixed integer linear program (MILP). This optimization is done over the target lifetime of the network and uses an optimal routing that assumes the knowledge of future solar insolation and traffic flows. This results in a lower bound on the network upgrade costs which is used as a comparison with real provisioning algorithms. A traffic growth provisioning algorithm is presented based on doing an iterative local optimization. A technique based on a genetic algorithm approach is then introduced for determining low cost node resource upgrading. Results are given which show that the genetic algorithm approach obtains the best results and performs favorably compared with the lower bound.

A review of the work related to each resource management problem is given in each chapter.

1.3 Thesis Organization

Chapter 2 introduces the background information related to the work in this thesis. Background information on Wireless Local Area Networks (WLANs) and Wireless Mesh Networks (WMNs) is presented. A survey of previous work that deals with power saving for wireless infrastructure networks is also presented.

In Chapter 3, results are presented for energy aware provisioning for solar powered wireless mesh nodes. A resource provisioning algorithm is proposed based on the use of

shortest-path routing and taking into account the node energy-flow for the target deployment time period. A genetic algorithm that incorporates energy-aware routing into the resource assignment procedure is then introduced. The results show the large cost savings that an energy aware resource assignment can achieve when compared to that done using the conventional methodology. To evaluate the quality of the resource assignments, a linear programming formulation is developed which gives a lower bound on the total network resource assignment.

Chapter 4 proposes a mechanism for achieving fair bandwidth control on a per-flow basis. A bound which achieves the best max-min fair bandwidth control subject to eliminating network outage is formulated. This bound uses knowledge of future solar insolation to determine the optimum bandwidth control. This bound motivates a proposed bandwidth control algorithm whose operation uses prediction based on access to on-line historical weather data. The results show that the proposed algorithm eliminates node outage and performs very well compared to the optimum bandwidth control bound for a variety of network scenarios.

In Chapter 5, traffic growth management in solar powered wireless mesh networks is addressed. A mixed integer linear programming (MILP) formulation is derived which is used to optimize the costs of node resource upgrades. Using this result, a lower bound on the network upgrade cost is obtained. The chapter then proposes the use of a genetic algorithm based methodology for determining practical cost-effective mesh node resource upgrading. Various results are given using networks with random, mesh and tree topologies which show the value of the proposed mechanism. In particular it was found that the genetic algorithm approach achieves results which are much better than those from an algorithm which uses local optimization. It also performs well compared to the derived lower bound.

The thesis is then concluded in Chapter 6.

Chapter 2

Background

2.1 Introduction

This chapter presents an overview of the background information and concepts relevant to the analysis of solar powered wireless mesh networks. The chapter starts by presenting background information on Wireless Local Area Networks (WLANs), Wireless Mesh Networks (WMNs) and their standards. It then surveys some initiatives relating to solar powered wireless infrastructure networks. Finally, current methodologies used to model solar powered systems are reviewed.

2.2 Wireless Local Area Networks

Wireless local area networks (WLANs) connect two or more devices using radio communications within a relatively small region, such as within the floor of a building or a campus. Wireless LANs have witnessed tremendous growth in recent years and have become one of the fastest growing segments in the telecommunications industry. They offer users many benefits such as portability, flexibility, increased productivity, and lower installation costs compared to wired networks. The first standard for WLANs was made in the late 1990's by the Institute of Electrical and Electronics Engineers (IEEE) 802.11 workgroup, and became the IEEE 802.11 standard. The next section reviews the IEEE 802.11 standard and some of its extensions.

2.2.1 IEEE 802.11 Standard

In 1997, the IEEE adopted the first IEEE 802.11 standard for WLANs (IEEE802.11, 2008). The standard defines a medium access control (MAC) sub-layer, MAC management protocols and services, and details of the physical (PHY) layers (Ergen, 2002). Supported

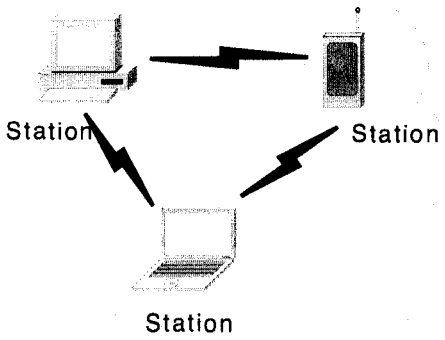

Figure 2.1: Independent Basic Service Set (IBSS)

services in the standard include authentication, privacy, and data delivery; these functions are typically embedded in the hardware and software of a network interface card (NIC) that is installed in the device that connects to the WLAN.

The IEEE 802.11 standard defines a Station (STA) as the component that connects to the wireless medium. The definition of stations does not distinguish between mobile or stationary devices. A Basic Service Set (BSS) is defined as a set of stations that communicate with one another. When all of the stations in the BSS are connected in a peer-to-peer fashion, the BSS is called an independent BSS (IBSS). An IBSS is typically a short-lived network that is established in an ad hoc manner with a small number of stations. A sample IBSS is shown in Figure 2.1 where three devices are communicating with each other using direct radio links.

When a BSS includes an access point (AP), it is called an infrastructure BSS. The AP acts as a central controller that organizes communications between stations. In this case, if one station must communicate with another, the communication is sent first to the AP, which then forwards it to the destination station. Figure 2.2 shows a sample infrastructure BSS consisting of the AP and 3 other stations. In this BSS, when Station 1 wants to communicate with Station 2, Station 1 transmits to the AP first and then the AP forwards the data to Station 2.

An Extended Service Set (ESS) is a set of infrastructure BSSs, where the APs forward traffic from one BSS to another to interconnect the BSSs and to facilitate the movement of stations between different BSSs. The APs perform this communication via an abstract medium called the distribution system (DS). To network equipment outside of the ESS, the ESS and all of its stations appear as a single MAC-layer network where all stations are physically stationary. Thus, the ESS hides the mobility of the stations from everything outside the ESS.

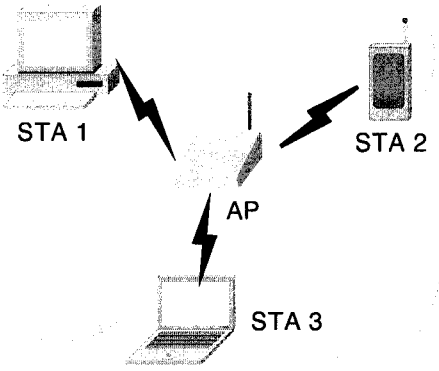

Figure 2.2: Infrastructure BSS (BSS)

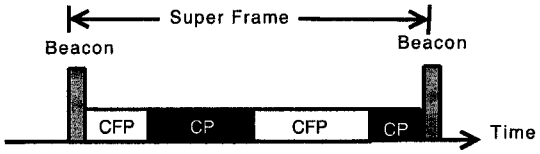

Figure 2.3: IEEE 802.11 Super Frame

In a BSS, transmissions from a station are broadcast on a shared transmission medium, and can be heard by all other stations. When two or more stations transmit simultaneously, their packets may interfere (collide), resulting in the loss of all involved transmissions. A medium access control (MAC) protocol is used to coordinate access to the shared medium. The primary function of the MAC protocol is to minimize collisions so that efficient use of the wireless medium is achieved.

In the IEEE 802.11 standard, time is divided into repeated periods, called superframes. As shown in Figure 2.3 a superframe starts with a beacon packet and is divided into a Contention Free Period (CFP) and a Contention Period (CP). The beacon packet is a management packet that synchronizes the local timers in the stations to the AP and delivers protocol related parameters. IEEE 802.11 defines two types of medium access control algorithms during the CFP and the CP periods, the Distributed Coordination Function (DCF) and the Point Coordination Function (PCF). During the CFP, the PCF is used for accessing the medium, while the DCF is used during the CP.

DCF works as a listen before-send protocol (Mangold *et al.*, 2002), based on Carrier

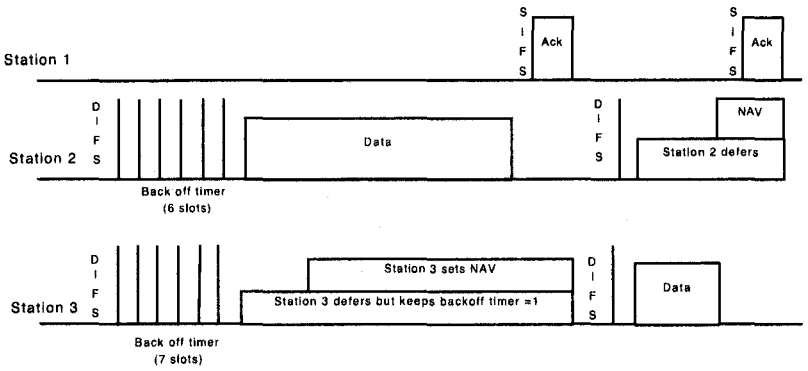

Figure 2.4: IEEE 802.11 timeline

Sense Multiple Access with Collision Avoidance (CSMA/CA). Carrier Sense Multiple Access is a probabilistic MAC protocol in which a node verifies the absence of other transmissions before transmitting. This is done by sensing the medium for the presence of a carrier signal from other stations (Ni *et al.*, 2004). Stations deliver packets after detecting that there is no other transmission in progress on the wireless medium.

The IEEE 802.11 standard defines another carrier sensing mechanism called virtual carrier sensing (Ergen, 2002). Virtual carrier sensing is optionally used by the transmitting station to inform all other stations in the same BSS of the duration of its transmission. Listening stations will not start any transmissions during this time by setting their Network Allocation Vector, NAV, timer to a value equal to the transmission duration.

The DCF mechanism is shown in Figure 2.4. As seen in the figure, Station 2 and Station 3 are contending for the medium. Once Station 2 and Station 3 detect an idle medium for a duration of a DCF inter-frame space (DIFS), they both wait for a random time before starting their transmission. The stations wait for this random time to avoid collisions. When Station 2 starts transmission, Station 3 sets its NAV timer to the transmission duration of Station 2. Moreover, it can be seen in the figure that acknowledgment packets are sent after the receiving station waits for a short inter-frame space (SIFS), whose duration is shorter than the DIFS. Varying inter-frame spacings create different priority levels for different types of traffic. Using this mechanism, high-priority traffic does not have to wait as long as low priority traffic after the medium has become idle. High-priority transmissions can begin once the SIFS has elapsed.

Priority-based access can also be used to access the medium using PCF. PCF is a synchronous service that implements a polling-based contention-free access scheme where the AP acts as a point coordinator (PC). In PCF, the PC polls a station, asking for pending data packets. If the PC receives no response from a polled station after waiting for a PCF Inter frame Space (PIFS), it continues polling other stations until the CFP expires. A specific

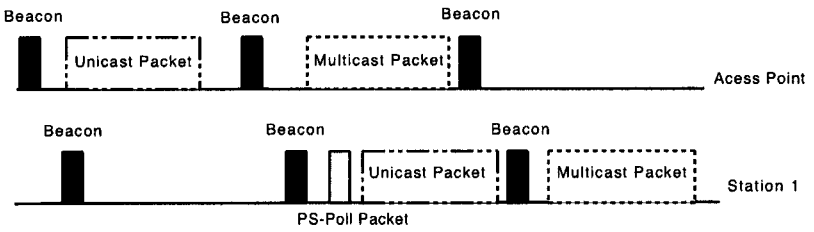

Figure 2.5: IEEE 802.11 power saving mode (simplified)

control frame, called CF-End, is transmitted by the PC as the last frame within the CFP to signal the end of the CFP.

Since many IEEE 802.11 stations run on battery power, the standard includes features that can be used (illustrated in Figure 2.5) to prolong the battery lifetime (Ergen, 2002). A station can be in one of two power modes, that is, the active mode when it can receive and transmit packets, and a power-save mode (PS) where it is in the sleep state, a state where it has turned off the receiver and transmitter to conserve power. The standard does not specify when a station may enter or leave a power save mode, only how the transition is to take place. In an infrastructure BSS, the power management mechanism is centralized in the AP. The AP assumes the burden of buffering incoming data and multicast packets for power saving stations and delivering them when the stations request their transmission. This allows the stations to remain in the power saving state for long time periods.

A station that wants to enter the power saving mode informs the AP of its listen period. The listen period is the number of consecutive inter-beacon frame intervals before a station must awaken to look for data that is held by the AP. The AP will hold packets destined for stations in the power saving mode for a minimum time not less than the listen period indicated in the station's request. The AP indicates awaiting packets using a traffic indication map (TIM) that is included within the beacons. The standard defines an aging algorithm to discard buffered packets, though a specific algorithm is not described.

When power saving is used, a station awakens at the expected time of a Beacon transmission to learn if there are any data packets waiting, and to inform the AP when the station will reenter the power saving mode. On receipt of an indication of awaiting packets at the access point, the station sends a PS-Poll packet to the access point and waits for a response in the active state. The access point responds to the poll by transmitting the pending packet or indication for future transmission. The access point indicates the availability of multiple buffered packets using the "More" data field in the frame control field of each packet. The station is required to send a PS-Poll to the AP for each data packet it receives with the "More" data bit set.

The station must also wake up at times determined by the AP, when multicast packets are to be delivered. This time is indicated in the beacon packets as the delivery traffic

indication map (DTIM). If an AP has any buffered multicast packets, those packets are sent immediately after the beacon announcing the DTIM (without an explicit PS-Poll from the station). If there is more than one multicast packet to be sent, the AP will indicate this fact by setting the "More" data bit in the frame control field of each multicast packet except for the last one sent.

Figure 2.5, illustrates the power saving mechanism used in the IEEE 802.11 standard. In the figure, the AP holds a unicast packet destined to Station1 which is in the power save mode. The AP indicates in the next beacon that it has a packet for Station 1. When Station 1 listens to the beacon, it sends a PS-Poll to the AP which then delivers the packet to the station. The AP holds any multicast packets for Station 1 since it is in the power save mode. The AP then indicates in the next beacon that it has a multicast packet and sends the packet without waiting for a PS-Poll from the station.

In a contention-free period (CFP) the AP will deliver buffered packets to stations that are CF-Pollable. The CFP may also be used to deliver multicast packets after the DTIM is announced.

IEEE 802.11e is an enhancement to the IEEE 802.11 standard which modifies the Media Access Control (MAC) layer to define a set of quality of service enhancements for wireless LAN applications. The standard is considered important for delay-sensitive applications, such as Voice over Wireless IP and Streaming Multimedia (IEEE 802.11e, 2005). IEEE 802.11e enhances the DCF and the PCF, through a new coordination function: the Hybrid Coordination Function (HCF). There are still two phases of operation within the superframes, i.e., a CP and a CFP. The contention-based channel access method Enhanced Distributed Channel Access (EDCA) is used in the CP only, while the HCF Controlled Channel Access (HCCA) that uses polling, can be used in both phases. Both EDCA and HCCA allow the assignment of low and high priority traffic to different Traffic Categories(TC). The EDCA gives high priority traffic a higher chance of being sent than low priority traffic by allowing stations with high priority traffic to wait a little less before sending their packets.

Each priority level is assigned a Transmit Opportunity (TXOP). A TXOP is a time interval during which a station sends as many packets as possible. This reduces the problem of low rate stations gaining an inappropriate amount of channel time in the legacy IEEE 802.11 DCF MAC.

The HCCA works like the PCF. However, during the HCCA, the AP can initiate polling at any time. This is called a Controlled Access Phase (CAP) in IEEE 802.11e. A CAP is initiated by the AP, whenever it wants to send or receive data in a contention free manner. The other difference with the PCF is the availability of traffic classes which means that the HC can give priority to one station over another, or adjust its scheduling mechanism in any way it wants. As in EDCA, the stations are given a TXOP selected by the HC.

IEEE 802.11e includes an Automatic Power Save Delivery (APSD) mechanism (Perez-Costa *et al.*, 2007). The main difference between the IEEE 802.11 standard power save

mode and APSD is that with APSD a station must be awake during a Service Period (SP). Two types of SPs are possible under APSD: unscheduled and scheduled. Unscheduled SPs (U-APSD) are defined only for stations accessing the channel using EDCA, while Scheduled SPs (SAPSD) are defined for both access mechanisms. As in the legacy IEEE 802.11 power save mode, the AP will buffer packets for a station in the power save mode for a period not less than the station's listen period.

The main idea behind the U-APSD design is to use data packets sent by power saving stations to the AP as indications of the instants when these stations are awake. When such an indication is received by the AP, the AP delivers any data packets that were buffered for the station while it was in sleep mode. In S-APSD the HC defines periodic service intervals which allow the synchronous delivery of traffic.

IEEE 802.11 does not include any native procedures that would allow an access point to achieve power saving, and this aspect of IEEE 802.11 is an impediment to the development of a real power saving WLAN infrastructure. In classical IEEE 802.11, power saving has dealt with end user stations since access points are assumed to have continuous power connections [IEEE Standard 802.11, Wireless LAN Medium Access Control (MAC) and Physical Layer Specifications, IEEE, 1997]. Several references in the literature have discussed this problem (Farbod and Todd, 2004), (Zhang *et al.*, 2004), (Li *et al.*, 2005), (Choi *et al.*, 2007) . In the next section wireless mesh networks will be introduced.

2.3 Wireless Mesh Networks

Wireless Mesh Networks (WMNs) extend the reach of wireless networks using multi-hop communications. A sample wireless mesh network that includes infrastructure connectivity is shown in Figure 2.6. The network consists of a number of stationary access points (mesh APs which may also be referred to as wireless relay nodes) and several wireless users (mesh clients) and gateways. In this architecture, mesh APs form an infrastructure for clients (Akyildiz *et al.*, 2005) and the gateways connect the mesh APs to the Internet. Dashed and solid lines in the figure indicate wireless and wired links, respectively. The mesh APs form a fully wireless backbone network which provides Internet connectivity to the users through the gateways. The WMN infrastructure/backbone can be built using various types of radio technologies, including IEEE 802.11.

Industrial standards groups are also actively working on new specifications for mesh networking. For example, IEEE 802.11 (IEEE802.11, 2008) , IEEE 802.15 (IEEE802.15, 2008) , and IEEE 802.16 (IEEE802.16, 2008) all have established sub-working groups to focus on new standards for WMNs.

In many WMN applications, radio coverage is required over expansive outdoor areas where the mesh nodes can be operated using an energy sustainable source such as solar power. For this reason, mesh APs require power management to optimize both power

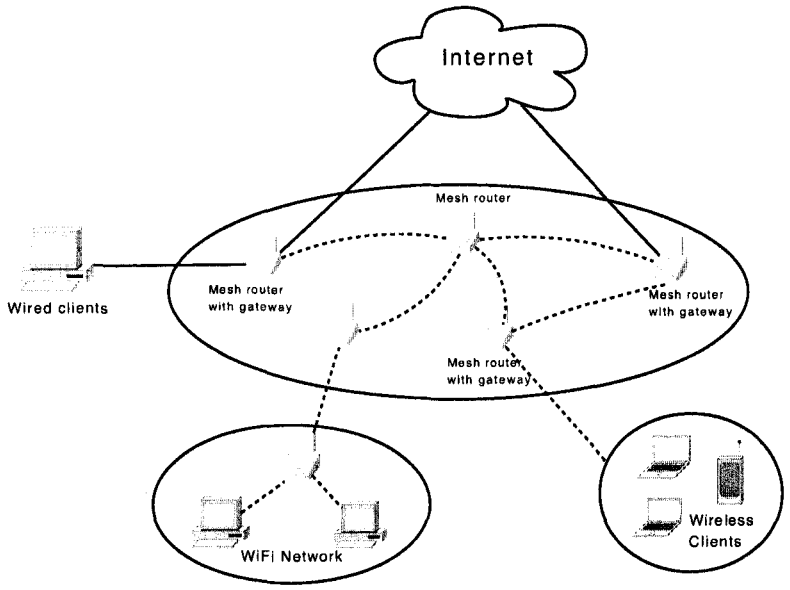

Figure 2.6: Wireless mesh network example

efficiency and network connectivity. In the next section, some solar powered IEEE 802.11 WLAN mesh network initiatives will be reviewed.

2.4 Solar Powered Wireless Mesh Networks

2.4.1 Power Savings in Infrastructure Wireless Mesh Networks

In infrastructure-based wireless networks, the infrastructure nodes (e.g., mesh APs) are usually powered from a continuous energy source. For this reason, mesh APs do not have a constraint on power consumption and power management in the mesh APs aims to control interference (Krishnamurthy, 2004), spectrum spatial-reuse, and topology (Li *et al.*, 2002). Only recently, various research and commercial activities have included power saving in the mesh APs. In this section some recent solar powered IEEE 802.11 WLAN mesh network initiatives are discussed.

Solar powered wireless mesh networks are starting to appear in many Wi-Fi infrastructure scenarios (Todd *et al.*, 2008). For example, the city of Minneapolis has deployed a solar powered Wi-Fi network as a part of the ParkWiFi project, which consists of more than 400 APs (Park WiFi Project, 2007). A solar powered wireless Internet access network

has recently been deployed at the Pearl Street Mall in Boulder, Colorado with the cooperation of Lumin Innovative Products (Lumin Innovation Products Inc, 2007). Inveneo, a non-profit organization, currently offers solar powered wireless networks in the developing world (Inveneo, 2007). Meraki has plans for deploying a solar powered outdoor Wi-Fi mesh node (Meraki Outdoor) (Meraki, 2007), and IR Data Corporation provides a solar powered Wi-Fi AP that includes a 900 MHz radio mesh router (IR Data Corporation, 2007). An example of this is the Battery Operated Systems for Community Outreach (BOSCO) initiative, which is expected to provide Internet services for displaced people in northern Uganda (BOSCO, 2007). In addition, the One Laptop Per Child (OLPC) project includes the use of a solar powered IEEE 802.11 WLAN mesh repeater. These devices can be easily mounted to provide WLAN mesh coverage for OLPC users. The Green Wi-Fi initiative also provides solar powered access for developing countries (Green WiFi, 2007).

A common issue in practical solar powered WLAN infrastructure is the excessive cost of the solar panel and battery components, especially in temperate geographic regions. This provisioning cost is closely tied to the power consumption design profile of a given mesh node. In a multi-radio solar powered node design, this cost can be reduced by operating the relay radios (i.e., those that communicate only between mesh APs) using some form of power save mode. Although an IEEE 802.11 standard does not as yet exist for this, the IEEE 802.11s activities plan to include this option (Camp and Knightly, 2008). Unfortunately, many solar-powered applications involve single radio nodes, in either low usage applications or in hybrid solar/non-solar networks. Relay-link power saving clearly does not apply to this case; thus, the provisioning cost of these types of nodes is often far higher than necessary.

Very minor modifications to the IEEE 802.11 standards would open the door to significant solar node cost reductions if AP power saving were permitted. It was shown in (Farbod and Todd, 2004) that WLAN mesh APs which operate using a sustainable energy source can benefit greatly from protocol-based power saving features. Currently, however, IEEE 802.11 does not provide a mechanism for placing APs into a power saving mode. The proposed modifications to the IEEE 802.11 standards to allow AP power savings are now briefly reviewed.

The work in (Zhang *et al.*, 2004), and (Li *et al.*, 2005) propose extensions to IEEE 802.11 and IEEE 802.11e to include power savings on the access point. In (Zhang *et al.*, 2004) the authors present a power saving access point (PSAP) that is backward compatible to a wide range of legacy IEEE 802.11 end stations and existing wired access points. The PSAP is designed so that it can perform dual-channel multi-hop relaying, and at the same time accommodate conventional Wi-Fi compliant IEEE 802.11 end stations, without any modification to existing mobile stations. This is done using two channels: a HOME channel (H-channel) and a RELAY channel (R-channel). The PSAP uses the H-channel to act as an access point for mobile stations (MSs) within its coverage range and the R-channel to forward/download traffic to/from its parent AP or PSAP. To reduce cost and

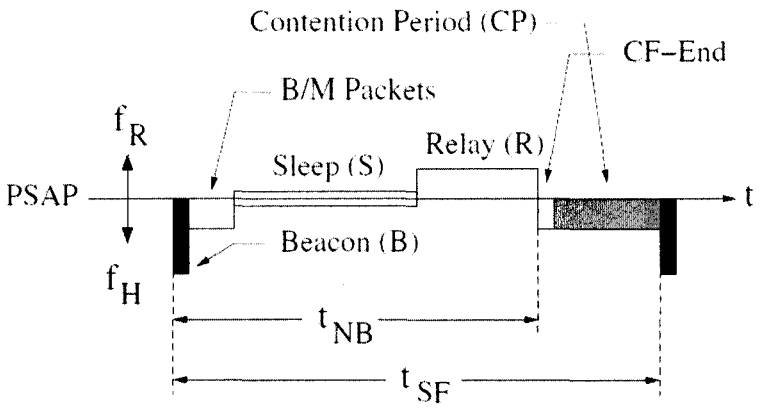

Figure 2.7: Power Saving AP Operation (Zhang *et al.*, 2004)

power consumption, each PSAP has only a single IEEE 802.11 wireless interface.

Figure 2.7 illustrates the operation of the PSAP. As in conventional IEEE 802.11, the PSAP establishes a superframe of length t_{SF} , which can span multiple beacon intervals. The superframe timeline consists of three subframes, the Sleep/Doze or S subframe, the Relay or R subframe, and the contention period, CP, subframe. During the S subframe, the PSAP is sleeping with its radio and potentially other subsystems switched into a lower power conserving state. In the R subframe, the PSAP has its radio tuned to the R-channel, and is relaying traffic to/from its upstream neighbor. In the CP subframe, the PSAP has its radio tuned to the H-channel and traffic is passed between the PSAP and MSs using the normal IEEE 802.11 infrastructure based DCF procedures. The authors use a NAV-blocking mechanism to organize access to the PSAP. In the NAV-blocking scheme, the beacon transmitted at the start of the superframe advertises the PSAP as an IEEE 802.11 point coordinator (PC). It also specifies a PCF period of duration equal to the sum of the S and R subframes. This action serves to block all stations from accessing the H-channel for this duration since MSs will set their NAV to this value. Once this has been done, the PSAP is then free to sleep and switch to the R-channel. At the end of the R subframe, the PSAP transmits a CF-End packet on the H-channel to signify the beginning of the CP subframe.

The authors in (Li *et al.*, 2005) extend the IEEE 802.11/ IEEE 802.11e MAC protocol to accommodate power saving in the AP by generalizing the NAV concept to that of a Network Allocation Map or NAM. For a given AP, a NAM specifies one or more future non-overlapping time periods during the inter-beacon interval when an AP's channel is unavailable for transmission activity. During the NAM intervals the AP radio may be either in a low power doze mode or it may be relaying traffic on a different channel. Figure 2.8 shows an example of a network with 2 APs (MAP_1 and MAP_2), where the first line shows

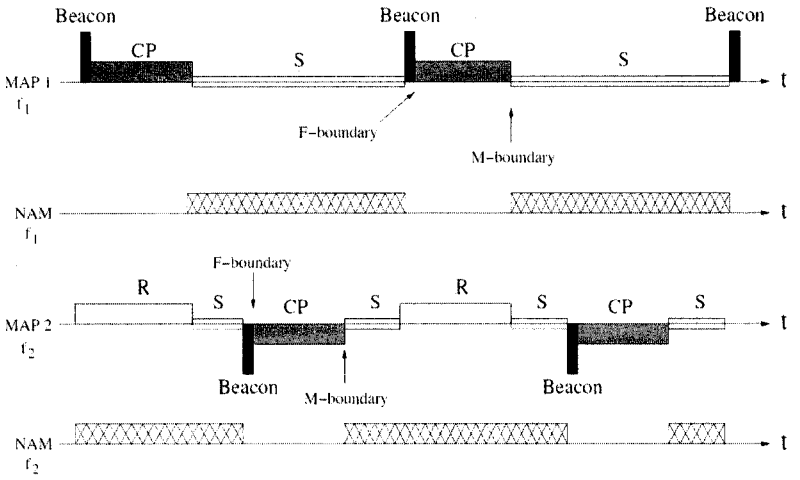

Figure 2.8: NAM Power Savings (Li *et al.*, 2005)

the AP activities and the second line shows the NAM associated with this AP. In Figure 2.8, S indicates that the AP is in sleep mode, CP represents a contention period and R indicates that the AP is relaying traffic on a different channel. Each NAM entry start and end time also includes a boundary type, which is either fixed (an F-Boundary) or movable (an M-Boundary). An F-Boundary type is one where the transition to the new subframe type is guaranteed to occur at that point in the superframe. An M-Boundary is different in that it can be changed on a dynamic basis by the AP from one superframe beacon interval to the next to accommodate traffic conditions, and is advertised in the most recent beacon.

Having surveyed different power saving techniques, it is important to gain a thorough understanding of how renewable energy systems are modeled in practice. In the following section, a detailed description is provided.

2.5 Solar Conversion

Knowledge of the quantity of solar energy available at a specific location is of prime importance for the design of any solar energy system. Although the solar radiation is relatively constant outside the earth's atmosphere, local climate influences can cause wide variations in available insolation on the earth's surface. Due to the earth's rotation, asymmetric orbit about the sun, and the contents of its atmosphere, a large fraction of the solar energy does not reach the ground. The rate at which solar energy reaches a unit area at the earth is called the "solar irradiance" or "insolation". The units of measure for irradiance are watts per square meter (W/m^2).

Solar irradiance is an instantaneous measure of rate and can vary over time. These

variations have a strong deterministic component but processes such as air humidity, pressure and cloud cover induce randomness into the received insolation. The modeling of the above processes is mainly done using stochastic processes because they are too complicated to be studied using deterministic models. As solar radiation passes through the earth's atmosphere, it is absorbed, reflected, and scattered.

In this thesis the term "direct" will be used to represent solar irradiance coming directly from the sun, and the term "diffuse" will be used to indicate solar irradiance coming from all other directions. The daily total radiation incident on a tilted surface, G_t, is composed of direct, G_b, ground reflected, G_r, and sky-diffuse, G_d, components, i.e.,

$$G_t = G_b + G_d + G_r, \tag{2.1}$$

where G_b represents the irradiance coming directly from the sun, G_d represents the diffuse radiation falling on a tilted surface, and G_r is the solar energy reflected from surrounding surfaces. The calculation of the direct component is a straightforward geometric problem (Klein, 1977). However, the diffuse component estimation requires a complex computation and the most widely used method will be described later. Since the ground-reflected component is highly site-dependent and doesn't significantly contribute to the total, it is usually ignored (Perez and Stewart, 1986). The calculation of G_b, G_d and G_r is now explained.

2.5.1 The Incidence angle

The incidence angle, θ, is the angle at which the solar radiation strikes the panel. This angle determines the energy received by the panel and is mainly a function of the position of the sun in the sky, and the slope and orientation of the panel. Several parameters are used to calculate these two factors: the solar declination angle, the hour angle, and the zenith angle. The solar declination angle is the angle between a plane perpendicular to the solar radiation and the axis of rotation of the earth. It can be calculated as follows (Klein, 1977).

$$\delta = 23.45^\circ \cdot sin[360(284 + n)/365], \tag{2.2}$$

where n is the Julian day [1 ... 364]. The hour angle represents the angular distance that the earth has rotated in a day and can be expressed as,

$$h = 15(t_s - 12), \tag{2.3}$$

where t_s is the number of hours from local solar noon. The zenith angle is the angle between the solar radiation beam and a line perpendicular to the panel location. It can be computed as follows,

$$cos(\theta_z) = sin(\phi)sin(\delta) + cos(\phi)cos(\delta)cos(h), \tag{2.4}$$

where ϕ is the location's latitude.

2.5.2 Direct Solar Insolation

The direct solar insolation component is calculated using Kleins method (Klein, 1977). This method is widely used because of its relative simplicity, as it requires only daily global insolation on a horizontal plane (Kamali *et al.*, 2006). Klein computed the direct component of solar radiation on a tilted plane as a function of the direct normal solar radiation and the incidence angle. In solar powered WLAN mesh applications, the solar panels are pointed directly south and sloped slightly greater than the geographic latitude (in the northern hemisphere) so that solar absorption is highest during winter months. For these panels the incidence angle is given as

$$cos(\theta) = cos(\phi - \beta)cos(h)cos(\delta) + sin(\phi - \beta)sin(\delta), \tag{2.5}$$

where ϕ is the location's latitude and β is the solar panel's slope. This can be simplified further for the case where the tilt angle is equal to the value of the latitude,

$$cos(\theta) = cos(h)cos(\delta). \tag{2.6}$$

This means that the solar incidence angle for an equator-facing plane is only a function of the hour angle and the declination angle. Now, the direct component of solar radiation can be written as

$$G_b = G_{b,n} \cdot max[0, cos(\theta)], \tag{2.7}$$

where $G_{b,n}$ is the normal beam irradiation which can be obtained from The Meteorological Service of Canada. The reason behind taking the maximum of zero and $cos(\theta)$ is that during the night, the unmodified equation is not correct.

2.5.3 Diffuse Solar Insolation

Diffuse radiation does not come directly from the sun and its strength is a function of sky clearness and brightness. The widely accepted Perez model for estimation of the diffuse component of solar irradiance on tilted planes (Perez and Stewart, 1986) is now described. The diffuse solar insolation on a titled surface G_d can be given by (Soga *et al.*, 1999).

$$G_d = G_{d,h}F, \tag{2.8}$$

where $G_{d,h}$ is the horizontal diffuse irradiation which can also be obtained from The Meteorological Service of Canada and F is the function representing the proportion of diffuse irradiation on tilted surfaces to horizontal diffuse irradiation. To calculate F, Perez defines

3 basic components that parameterize all the solar insolation conditions from overcast to clear. These components are

1. The solar zenith angle θ_z.
2. The sky clearance noted as ϵ, which is given by

$$\epsilon = \frac{(G_{d,h} + G_{b,n})/G_{d,h} + k\theta_z^3}{1 + k\theta_z^3}, \tag{2.9}$$

   where $G_{d,h}$ is the horizontal diffuse irradiance, $G_{b,n}$ is the normal incident direct irradiance, k is a constant equal to 1.041 for θ_z in radiance and the θ_z^3 formulation is added to eliminate the dependence of this component on the zenith angle.
3. The sky brightness Δ is calculated as

$$\Delta = G_{d,h}m/I_0, \tag{2.10}$$

   where m is the relative optical air mass (Kasten, 1996) and I_0 is the extraterrestrial irradiance.

Now the diffuse component on a tilted surface can be given as,

$$G_d = G_{d,h}[(1 - F_1)(1 + cos\beta)/2 + F_1 a/b + F_2 sin\beta], \tag{2.11}$$

where $a = max(0, cos\theta)$ and $b = max(0.087, cos(\theta_z))$. Based on the category into which the current sky's clearness index ϵ falls, the values of F_1 and F_2 can be obtained by looking up Table 6 in (Perez *et al.*, 1990).

The conversion algorithm can now be summarized as follows,

1. Estimate the direct component
   (a) Calculate the hour angle h according to Equation 2.3.
   (b) Calculate solar declination angle δ according to Equation 2.2.
   (c) Calculate θ according to Equation 2.5.
   (d) The direct component can be estimated using

$$G_b = G_{b,n} \cdot max[0, cos(\theta)]. \tag{2.12}$$

2. Estimate the diffuse component
   (a) Calculate the solar zenith angle θ_z using Equation 2.4.
   (b) Calculate the sky clearance index ϵ using Equation 2.9.

(c) Using ϵ look up the values of F1 and F2 from Table 6 in (Perez *et al.*, 1990).

(d) The diffuse component can be estimated as

$$G_d = G_{d,h}[(1 - F_1)(1 + cos\beta)/2 + F_1 a/b + F_2 sin\beta]. \quad (2.13)$$

3. The total irradiance on a tilted plane is

$$G_t = G_b + G_d. \quad (2.14)$$

2.6 Conclusions

In this chapter a review of the necessary background information has been presented. The discussion began by presenting an overview of Wireless Local Area Networks (WLANs) and Wireless Mesh Networks (WMNs) including a summary of the most relevant features of the IEEE 802.11 standard. A survey of previous initiatives relating to power saving in wireless infrastructure networks was given. This was followed by reviewing the current methodologies used to model received solar insolation based on available meteorological records.

In the next chapter, the problem of resource provisioning in solar powered wireless mesh networks is addressed. A mathematical formulation for the resource provisioning problem is given to obtain a lower bound that can be used to investigate the quality of resource provisioning mechanisms. A flow-based provisioning procedure is introduced which is motivated by conventional single-system photo-voltaic provisioning. This motivates the idea of incorporating energy-aware routing into the provisioning process. A unique resource provisioning mechanism which takes energy aware routing into account is then introduced. A genetic algorithm is developed for determining these resource assignments and the presented results show the significant cost savings that are possible using this approach.

Chapter 3

Energy Aware Provisioning in Solar Powered Wireless Mesh Networks

3.1 Introduction

Before a solar powered wireless mesh network is installed, the nodes must be provisioned with a solar panel and battery combination that is sufficient to accommodate the anticipated network bandwidth flow profile. The assigned configuration for each node must be such that the network survives without node outage for the desired deployment duration. This is normally done by assuming a temporal load profile for each node, and then by assigning resources that are based on results obtained using historical meteorological data for the geographic location where the network is to be deployed (Farbod and Todd, 2006). Unfortunately, this methodology requires that the network bandwidth flow assignment be determined before the nodes are provisioned, and thus it does not give a resource provisioning which can take into account the use of energy aware routing. Intuitively, a network which uses energy aware routing should be able to avoid outage using node provisionings which are less costly than in the conventional resource provisioning case. For this reason, the cost of node provisioning may be unnecessarily high when conventional resource assignment is used.

In this chapter this node energy provisioning problem is considered. First the problem is formulated with the objective of minimizing the network resource provisioning cost. A methodology for determining this resource assignment is then introduced which uses solar insolation history and a target bandwidth flow profile as inputs. This is referred to as Shortest Path Resource Provisioning (SPRP). A methodology for mesh node resource provisioning is then introduced which incorporates the use of energy aware routing. The objective is to obtain a minimum total network cost resource assignment, subject to satisfying the target load profile, and accounting for the desired geographic deployment location. A genetic algorithm (GA) is then proposed for determining this energy provisioning. Results

are presented which show the large resource savings that energy aware resource assignment can achieve when compared to that done using a conventional resource assignment. A linear programming formulation is also developed which gives lower bounds on the node resource cost assignments. A hybrid network case, where some of the deployed nodes have a continuous powered source is also included in our work.

3.2 Background

An objective in the design of most photo-voltaic (PV) systems is to ensure that the solar panel and battery resources are sufficient to provide an uninterrupted source of power. Methodologies for accomplishing this have been considered in the past literature, and will be briefly summarized.

In (Narvarte and Lorenzo, 2000) it was shown that the accuracy of different PV sizing methods are bounded by statistical laws, and that exceedingly complex methods are not needed for sizing PV systems. In (Maghraby *et al.*, 2002) three different methods for sizing PV systems were compared. The results show that the best provisioning can be obtained by simulation using historical solar insolation data. Based on these results most PV sizing papers use simulations to model hourly solar insolation data. This approach is reasonable since the provisioning process is normally done long before the PV system is deployed.

A deterministic analysis that produces the optimal design for a hybrid power system for either autonomous or grid-linked applications has been proposed in (Chedid and Rahman, 1997), and in (Borowy and Salameh, 1996) a methodology for calculating the optimum battery and PV array size for a stand alone hybrid (Wind/PV) system was developed. Long term data for wind speed and solar irradiance for every hour over 30 years were used to perform the provisioning. This data was used to compute the average power generated by the wind turbine and the PV module for each hour. For a given load characteristic, wind turbine, and a desired outage probability, an optimum number of batteries and PV modules was determined so that energy provisioning cost was minimized. Rather than assuming a constant system load, reference (Saengthong and Premrudeepreechacharn, 2000) takes variable energy loading into account in the sizing of solar powered systems.

In (Farbod and Todd, 2006) the design of solar powered WLAN mesh networks was considered from a resource allocation and outage control viewpoint. Algorithms were proposed which can prevent node outage by introducing a bandwidth deficit when the node battery energy drops below a pre-computed threshold. In this way, outage is avoided by adaptively reducing the level of service offered to the end user stations. In (Xu *et al.*, 2005), genetic algorithms are used to find the optimal resource assignment for a hybrid power system. This reference defines a mixed multiple-criteria integer programming problem which optimizes the types and sizes of wind turbine generators, the tilt angles and sizes of PV panels, and the battery capacities. The objective is to minimize the total cost, subject

to a power supply outage probability. In (Lopez and Agustin, 2005) a hybrid optimization using genetic algorithms was proposed to design a PV-Diesel system. The algorithm obtains the optimal configuration of PV panels, batteries and diesel generator, and minimizes the total net cost over the useful lifetime of the system. Reference (Shahirinia *et al.*, 2005) presented a genetic algorithm that calculates the electrification costs (i.e., capital, replacement, operation and maintenance, and fuel costs) over a 20 year period for a stand-alone multi-source hybrid power system. In much of the previous work in this area, the PV system load demand is an input to the problem and therefore each node can be independently provisioned. This assumption may be less valid in certain solar powered mesh network scenarios since the load on the system may vary dynamically with the flow routing that is applied at a given time.

There has also been a lot of previous work on energy aware routing. For example, the problem of maximizing the network lifetime was studied in (Chang and Tassiulas, 2004) where the lifetime is defined as the time until the first node experiences outage. In (Li *et al.*, 2006) the problem of traffic oblivious energy aware routing was studied and an optimization problem was presented with the objective of minimizing the maximum network energy utilization. In (Lin *et al.*, 2005) a power-aware routing algorithm is presented for wireless networks with renewable energy sources. The proposed algorithm is shown to be asymptotically optimal when compared to the full knowledge case.

In addition to the above work, genetic algorithms (GAs) have been used to solve network routing problems. In (Riedl, 1998) a GA was presented where a set of node locations and a traffic requirement matrix is given. The algorithm then optimizes the link topology and the routing paths in accordance with the input costs, so the average end-to-end packet delay does not exceed a specified threshold. In (Sirikonda, 2007) a GA was introduced to solve the problem of a multi-objective route optimization. This work finds the best paths between the end nodes that minimizes the number of hops, the queueing delay, the total path distance, bit error rate, and maximizes the transmission bandwidth. Using variable length chromosomes, reference (Ahn and Ramakrishna, 2002) introduced a GA which solves the shortest path routing problem. However, to our knowledge GAs have not been used to perform PV resource assignment in the presence of energy aware routing. Most previous work has sized PV systems without taking into account the interdependencies between the load demand and the routing algorithm.

3.3 Solar Powered Mesh Network Resource Provisioning

A simplified version of a solar powered mesh node is shown in Figure 3.1. Each node may contain one or more radio interfaces and it is assumed the node uses power saving such as that described in (Farbod and Todd, 2004). The solar panel and battery are connected to the node through a charge controller which performs functions such as battery over- and

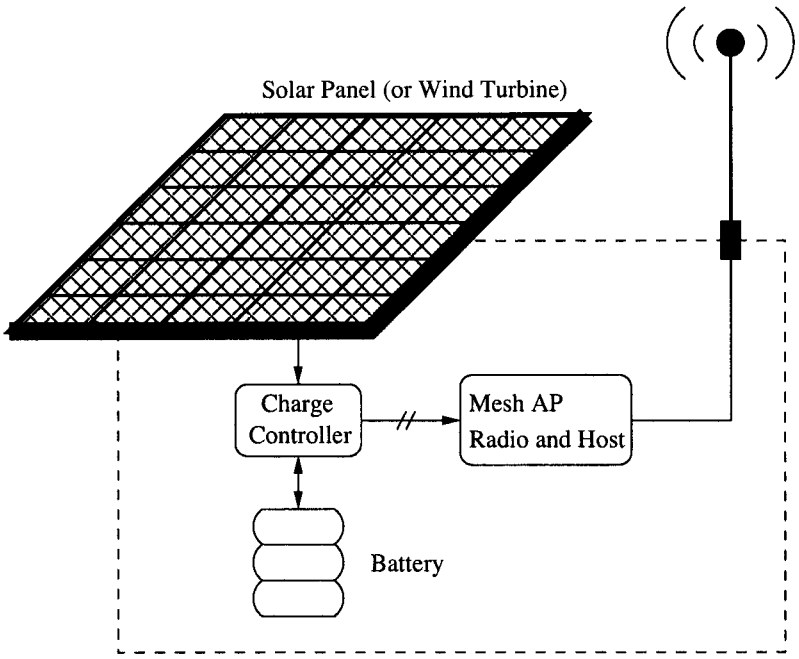

Figure 3.1: Solar Powered WLAN Mesh Node

under-charge protection. Photo-voltaic system modeling is normally done in discrete time and sufficient accuracy is obtained using the 1-hour Δ time increments method (Farbod and Todd, 2004). In the node energy flow model, $\mathcal{E}(i,k)$ is defined to be the energy per unit area produced in a solar panel for Node i over the time period $[(k-1)\Delta, k\Delta]$ and $P(i)$ is the assigned solar panel size. $B(i,k)$ is defined to be the battery energy stored in node i at time k, and $B_{max}(i)$ is defined to be the battery capacity. If $L(i,k)$ is assumed to be the load energy expended over the same period, then the energy flow equation can be written as (Safie, 1989)

$$B(i,k) = \min\{\max[B(i,k-1) + P(i)\mathcal{E}(i,k) - L(i,k), B_{outage}(i)], B_{max}(i)\}, \quad (3.1)$$

where $B_{outage}(i)$ is the maximum allowed depth of battery discharge based on safety and battery life considerations. Equation 3.1 is a simple recursion that finds the battery energy at time k to be that at time $k-1$, minus the load energy expended, and plus the energy received from the solar panel over that time period. When $B(i,k) \leq B_{outage}(i)$, the charge controller will disconnect the mesh node electronics and the node will experience a radio outage. The max/min operations in equation 3.1 take this into account and also define the battery capacity, $B_{max}(i)$.

Equation 3.1 can easily be modified to account for factors such as battery temperature

dependence. It is well known that both battery capacity and charging efficiency decrease with falling temperatures, and this effect should be accounted for in certain geographic locations (Farbod and Todd, 2004). In this case a tabular approach can be used so that when Equation 3.1 is evaluated, the current temperature acts as an index which returns factors that modify the battery capacity and charging efficiency. For simplicity in exposition, the form shown in Equation 3.1 will be used, but in the results temperature dependence will be accounted for when it is appropriate. The energy resource provisioning problem can now be stated.

3.3.1 Energy Provisioning Problem Statement

Resource provisioning involves the assignment of $\mathcal{P}(i)$ and $B_{max}(i)$ for each node, so that network outage is prevented. This is done using past solar insolation traces for the desired geographic deployment location, i.e., using sample functions of $\mathcal{E}(i,k)$ derived from recorded historical data.[1] The problem is as follows.

- The mesh network consists of N nodes modeled as a *directed graph* where each mesh node represents a vertex and two nodes can have an edge (i.e., a link) between them if they are within communication range. Each node is identified by an index in the set $\mathcal{N} = (1, 2, \ldots, N)$ and each edge is defined by an ordered pair (i, j) where $i, j \in \mathcal{N}$ are the transmitting and receiving nodes, respectively. The set of all edges is denoted by E. Traffic is relayed in a multi-hop fashion and a path from source to destination consists of one or more adjacent edges.

- Sample functions consisting of a bandwidth usage profile (BUP) and a solar insolation input trace are given for a contiguous deployment time period, $\mathcal{T}_{\mathcal{L}}$. The usage profile consists of a multi-commodity bandwidth usage matrix $\mathcal{M} = [m_{sd}(k)]$, where $m_{sd}(k) \geq 0$ indicates the aggregate bandwidth requirement from Node s to Node d during time period $((k-1)\Delta, k\Delta)$.[2] The solar insolation sample function consists of an input trace over the same time period whose values at Node i are given by $\mathcal{E}(i,k)$.

  The deployment time period is given by $\mathcal{T}_{\mathcal{L}} = (k_{min}\Delta, k_{max}\Delta)$ where k runs over the set $\mathcal{K} = (k_{min}, k_{min}+1, \ldots, k_{max})$.

[1] For the USA, this type of data is available from the National Renewable Energy Laboratory (NREL), U.S. Department of Energy, and for Canada it can be obtained from The Meteorological Service of Canada. These databases include solar insolation samples that span several decades of continuously collected measurements for hundreds of different geographic locations. Temperature samples are also included with the solar insolation traces.

[2] It is important to note that as in other resource provisioning problems, the BUP does not consist of individual user traffic flows. Rather, it is an aggregate loading profile that the network is designed to, based on the expected usage of the nodes and considering the experiences of the designers in past deployments. For this reason the bandwidth flows are allowed to be split over multiple network paths. This permits the required energy usage to be shared over multiple nodes if required.

- The objective is to assign $\mathcal{P}(i)$ and $B_{max}(i)$ so that the total solar panel and battery resource provisioning cost is minimized when Equation 3.1 is applied such that $B(i,k) > B_{outage}(i)$ for $k \in \mathcal{K}$ and $i \in \mathcal{N}$.

In order to generate practical resource provisionings, the sample function values must be provided to the system in a causal fashion so that future values are not known to the system as Equation 3.1 is evaluated.

Network deployments may be either permanent or temporary. In the permanent case, the deployment period may include all contiguous $\mathcal{E}(i,k)$ sample functions available for that geographic location. In the temporary deployment case, the network may only be required to operate over a specified time period, such as during specific months of the year. In this case, yearly solar cyclostationarity is assumed, and node provisioning is done using multiple $\mathcal{E}(i,k)$ sample functions covering the desired $\mathcal{T}_{\mathcal{L}}$ period in all previous years for which these records are available (Sayegh, 2008).[3]

Once the nodes are provisioned, the network can be deployed. A provisioning that satisfies the above problem does not guarantee that the network will be outage-free in the future, since the past data are only random sample functions of the BUP and the solar insolation processes. For this reason the derived provisionings are usually either increased by some safety factor (i.e., the open loop case), or, the nodes use some form of closed-loop outage control as discussed in (Farbod and Todd, 2006). Alternately, the safety factor margin can be incorporated into the BUP.

The resource provisioning problem is applicable to any geographic region. In some cases however, the practical motivation for an optimum battery and panel configuration is low. Results given in (Sayegh, 2008) show for example, that in the region around Phoenix, Arizona, daily solar insolation is so constant and plentiful that very small solar panel sizes and battery capacities will support typical mesh node configurations. The same study also shows that in more temperate regions, the cost of the panel and battery can be a significant fraction of the total node cost. In this case reductions in their size can have major business and deployment advantages. Rather than mixing results for different regions, in this chapter solar insolation traces from Toronto, Canada, are used which is typical of data for temperate continental regions (Sayegh, 2008).

In order to investigate the quality of various resource provisioning mechanisms, in the next section a lower bound on the minimum cost node configurations is derived. This bound is first compared with the SPRP Algorithm introduced in Section 3.4, and then it is used to motivate a more sophisticated energy-aware provisioning procedure, presented in Section 3.5.

[3]In many geographic locations, the provisioning for the permanent deployment case can be found by determining an appropriate temporary deployment provisioning (Sayegh *et al.*, 2008). In a temperate climate for example, a small period during winter months may dictate the provisioning needed for permanent outage-free operation.

3.3.2 Energy Resource Provisioning Bound

Given historical solar insolation data and a bandwidth profile as discussed in Section 3.3.1, a linear programming optimization is formulated to compute lower bounds on the battery capacity for each node, given that the solar panel size is pre-determined. The relation between the battery capacity and its cost is linear so by minimizing the required battery capacity the provisioning cost is minimized. The result comes from assuming a-priori knowledge of both solar and BUP input traces, and therefore the optimization gives a lower bound on the provisioning for any causal algorithm that operates using the same inputs. Our objective is to find the minimum battery capacities subject to satisfying the routing and battery constraints, i.e., an edge (i, j) can only be assigned to a bandwidth flow when the energy levels at Nodes i and j are above $B_{outage}(i)$. The bound applies to hybrid networks which contain a mixture of nodes operating from continuous power sources and those using solar power. The set of node indices for solar powered nodes is defined as $\mathcal{N}_s$, and those with continuous (i.e., infinite energy) power supply connections as $\mathcal{N}_\infty$, where $\mathcal{N} = \mathcal{N}_s + \mathcal{N}_\infty$. The optimization can be written as follows, and a discussion of the various terms is given afterwards.

$$minimize \sum_{i \in \mathcal{N}_s} B_{max}(i) + \lambda_1 \sum_{(i,j) \in E} \sum_{k \in \mathcal{K}} f_{ij}(k) \tag{3.2}$$

subject to the following constraints.

$$0 \leq f_{ij}(k) \leq f_{max}(i, j) \tag{3.3}$$

for all $(i, j) \in E, k \in \mathcal{K}$, and,

$$0 \leq B_{max}(i), \tag{3.4}$$

for all $i \in \mathcal{N}_s$.

$$\sum_{(i,l) \in E} f_{il}(k) + \sum_{d \in \mathcal{N}} m_{id}(k) = \sum_{(h,i) \in E} f_{hi}(k) + \sum_{s \in \mathcal{N}} m_{si}(k) \tag{3.5}$$

for all $i \in \mathcal{N}$ and $k \in \mathcal{K}$.

$$B(i,k) = \begin{cases} \infty, & i \in \mathcal{N}_\infty \\ \min\{\max[B(i,k-1) + \mathcal{P}(i)\,\mathcal{E}(i,k) - L(i,k), B_{outage}(i)], B_{max}(i)\} & i \in \mathcal{N}_s \end{cases} \tag{3.6}$$

for all $k \in \mathcal{K}$.

$$L(i,k) = (\sum_{(i,l)\in E} Rf_{il}(k) + \sum_{(i,l)\in E} T\alpha f_{il}(k) + \sum_{(h,i)\in E} Tf_{hi}(k) + \sum_{(h,i)\in E} R\alpha f_{hi}(k) + \sum_{(i,l)\in E} S(1 - f_{il}(k) - \alpha f_{il}(k)) + \sum_{(h,i)\in E} S(1 - f_{hi}(k) - \alpha f_{hi}(k)))\Delta, \quad \forall i \in \mathcal{N}_s, k \in \mathcal{K}. \quad (3.7)$$

In constraint 3.3, $f_{ij}(k)$ represents the total bandwidth load on the edge between Node i and Node j at time k i.e., if $f_{ij}(k) \geq 0$ then edge (i,j) is on the available paths at time instance k, otherwise $f_{ij}(k) = 0$. Constraint 3.3 is the normalized link (edge) capacity constraint which ensures that assigned bandwidth flows do not exceed the link capacity. In this constraint, $f_{max}(i,j)$ represents the maximum utilization capacity allowed on edge (i,j). Channel allocation is assumed to be done before the resource provisioning so $f_{max}(i,j)$ is calculated according to interference constraints. Constraint 3.4 sets a lower bound for the battery capacity and Constraint 3.5 ensures flow continuity across the nodes by ensuring that the input flow for each node is equal to its output flow. Equation 3.6 is the battery energy flow recursion taken from Equation 3.1 except that it assigns an infinite energy level to continuously powered nodes, i.e., $i \in \mathcal{N}_\infty$. Constraint 3.7 computes the total energy for each node over the current Δ interval. It is assumed that a power saving media access control protocol is used such as that described in reference (Farbod and Todd, 2006). Accordingly, the power consumption while transmitting a packet is denoted by T, while receiving a packet is denoted by R, and while in a power saving sleep mode is S. The second term in Line 1 of Equation 3.7 and the first term in Line 2 are the energies associated with ACKs and other associated reverse-link flows where α is a fraction that represents the reverse traffic, while the second term in Line 2 and Line 3 computes the energy consumed in power save mode. The first term in the objective function (i.e., Equation 3.2) minimizes the network cost by minimizing the required battery capacity. The second term is included in the objective function to find the minimum battery capacity solution that also minimizes the aggregate load on each node. This term is used to ensure that the optimizer solution will result in loop-free flow routing assignments. If this term is not included, the optimization may route bandwidth through loops if the nodes on the loop have extra energy. This will not affect the minimum battery capacity assignment, but the optimizer will return invalid flow routings.

The objective function and all the constraints are linear except for Constraint 3.6. The above optimization problem is simplified to an LP problem by introducing a new variable, $s(i,k)$, which serves a dual purpose. It is used to represent the surplus energy received by the system that cannot be stored by the battery and it can take a negative value when the

battery charge is found to be negative. Therefore, the following equations can be used

$$B_{outage}(i) \leq B(i,k) \leq B_{max}(i), \tag{3.8}$$

and

$$B(i,k) + s(i,k) = B(i,k-1) + \mathcal{P}(i)\,\mathcal{E}(i,k) - L(i,k). \tag{3.9}$$

for all $i \in \mathcal{N}_s, k \in \mathcal{K}$. Defining $B'(i,k) = B(i,k-1) + \mathcal{P}(i)\,\mathcal{E}(i,k) - L(i,k)$, i.e., the right hand side of Equation 3.9, $s(i,k)$ is given by

$$s(i,k) = \begin{cases} B'(i,k) - B_{outage}(i) & \text{if } B'(i,k) < B_{outage}(i) \\ B'(i,k) - B_{max}(i) & \text{if } B'(i,k) > B_{max}(i). \\ 0 & \text{otherwise} \end{cases} \tag{3.10}$$

Constraint 3.8 will replace the min max in equation 3.6 by setting the lower and upper bounds for the energy levels in the batteries. The second branch in Equation 3.6 will be replaced by Equation 3.9 which represents the solar node battery constraints and captures the energy replenishment. The absolute value of s should be minimized for all cases except when the non-linear constraint is active. Therefore, the objective function can be re-formulated as follows,

$$minimize \sum_{i \in \mathcal{N}_s} B_{max}(i) + \lambda_1 \sum_{(i,j) \in E} \sum_{k \in \mathcal{K}} f_{ij}(k) + \lambda_2 \sum_{k \in \mathcal{K}} \sum_{i \in \mathcal{N}_s} |s(i,k)|, \tag{3.11}$$

where λ_1 and λ_2 are control factors that are set so as to not interfere with the operation of the original objective. These control factors are chosen by trial and error.

The above development finds a bound on the total allocated battery capacity and will in general assign different battery capacities to each node. In some cases it may be desirable to assign the same battery capacity to all nodes. A solution for this case can be obtained by setting all $B_{max}(i) = B_{max}$ in the above optimization. It also generates routing that assumes a perfect knowledge of future bandwidth flows and future solar insolation. This provides a lower bound for any methodology that uses realizable algorithms. In the remainder of the paper this bound is used for comparisons with the practical resource assignment algorithms defined in Sections 3.4 and 3.5.

3.4 Shortest Path Resource Provisioning (SPRP)

In this section a resource provisioning mechanism (SPRP), based on using conventional flow routing for assigning the bandwidth usage flows is presented. The methodology is motivated by that used in conventional single-node resource provisioning (Farbod and Todd,

Algorithm 1 SPRP

for all $k_{min} \leq k \leq k_{max}$ **do**
Given the bandwidth usage matrix, $\mathcal{M}$, use Dijkstra's Algorithm to assign bandwidth flows at time $k\Delta$ using a hop-count link metric and subject to Equations 3.12 and 3.13.
end for
for all $i \in \mathcal{N}_s$ **do**
Provision each Node i using the resulting $L(i,k)$ for all $k \in \mathcal{K}$ from above, the solar insolation trace $\mathcal{E}(i,k)$ for all $k \in \mathcal{K}$, and the search procedure discussed in Sayegh (2008).
end for

2006). In the single-node case where the solar insolation and bandwidth load sample functions are given, then the procedures discussed in (Sayegh, 2008) can be used to obtain the optimum resource configuration. The minimum cost resource configuration can be found using a 1-dimensional gradient search which simulates the system using Equation 3.1. The search iterates on the assigned resources until the optimal value is obtained.

The SPRP Algorithm is shown in Algorithm 1. At each time epoch, shortest-path routing is assumed for the bandwidth flows using Dijkstra's Algorithm, and the link flows are computed such that

$$0 \leq f_{ij}(k) \leq f_{max}(i,j) \tag{3.12}$$

for all $(i,j) \in E, k \in$ K, and,

$$\sum_{(i,l)\in E} f_{il}(k) + \sum_{d\in\mathcal{N}} m_{id}(k) = \sum_{(h,i)\in E} f_{hi}(k) + \sum_{s\in\mathcal{N}} m_{si}(k), \tag{3.13}$$

where $f_{ij}(k)$ represents the sum of all flows routed through Edge (i,j) at time k. Equation 3.12 requires that the flows do not exceed some reasonable fraction, $f_{max}(i,j)$, of the normalized link capacity. As stated before the value of $f_{max}(i,j)$ is set according to the channel allocation that is done before the resource provisioning. Equation 3.13 ensures flow continuity for each node. In practice a link may not be utilized to its maximum capacity due to interference constraints or other reasons. f_{max} is added to capture these constraints on utilizing link capacities. When applying Dijkstra's Algorithm, if a given bandwidth flow cannot be routed without satisfying Equation 3.12, then the flow is split into two separate flows which are each then routed separately. Note that the flow routing is updated during each new Δ time epoch and the flow splitting is as discussed above and is often assumed (Huang and Peng, 2008).

As shown in Algorithm 1, once the set of $f_{ij}(k)$'s are obtained, the timeline of each node is then independently simulated using the energy flow balance from Equation 3.1

and the solar insolation input traces for the deployment location. Each node has an initial battery energy, $B(i, k_{min})$, where $i \in \mathcal{N}$. During this procedure the battery energy at each node is updated using Equation 3.1 and

$$L(i,k) = (\sum_{(i,l)\in E} Rf_{il}(k) + \sum_{(i,l)\in E} T\alpha f_{il}(k) + \sum_{(h,i)\in E} Tf_{hi}(k) + \sum_{(h,i)\in E} R\alpha f_{hi}(k) + \sum_{(i,l)\in E} S(1 - f_{il}(k) - \alpha f_{il}(k)) + \sum_{(h,i)\in E} S(1 - f_{hi}(k) - \alpha f_{hi}(k)))\Delta \quad \forall i \in \mathcal{N}, k \in \mathcal{K}. \quad (3.14)$$

Equation 3.14 computes the total energy for each node over the current Δ interval as in Equation 3.7. Given the bandwidth profile, network lifetime $\mathcal{T}_{\mathcal{L}}$, and the solar insolation data traces, shortest path (minimum hop count) routing is computed at each Δk time increment using Dijkstra's Algorithm with hop-count as the edge cost. After calculating the path the load on every node is updated according to the bandwidth flows as indicated in Equation 3.14. Once the temporal loading profiles have been determined, then each node is provisioned using the single-node procedures discussed above and in (Sayegh, 2008). In a practical system the battery capacities and panel sizes obtained may be rounded up to the nearest commercially available size.

The hybrid network case is also considered, where there is a mixture of solar powered nodes and those with continuous power connections. To assign battery capacities, shortest path routing using Dijkstra's Algorithm, is computed at each time increment. A value of d_s is chosen as the node cost for each solar powered node. Another value d_c is chosen as the node cost for each a continuous power nodes, and $d_c < d_s$. The edge costs are calculated by summing the node cost at each end of the edge. So links connecting two solar powered nodes have an edge cost equal to $2d_s$, while links connecting two continuously powered nodes have an edge cost equal to $2d_c$. Links connecting one node solar powered and one node continuously powered has an edge cost equal to $d_c + d_s$. This causes the routing algorithm to strongly favor continuously powered nodes. After computing the flows, the load on each node is updated as in Equation 3.14. Then the battery charge for solar powered nodes is updated according to Equation 3.1. Taking the load on each node individually, the same resource provisioning procedure as discussed in the all-solar case is followed.

It can be seen that SPRP inherits certain resource provisioning optimality from the single node case. Provided that the algorithm that routes the bandwidth flows is based solely on the usage matrix flow inputs given by $\mathcal{M}$, and is completed before the provisioning step occurs (as in Algorithm 1), then the total network cost will be minimum for that set of flow assignments.

Average Load (W)	SPRP (CAD)	Lower Bound (CAD)	Savings (%)
1	219	97	56
2	375	186	51
4	674	373	45
6	981	573	42

Table 3.1: Resource Assignment Cost vs. Average Load

3.4.1 SPRP Results Example

In this section some example results are presented which are representative of the performance of the SPRP resource assignment algorithm. A square 9-node mesh is considered and physical parameters based on IEEE 802.11 radio interfaces (Sayegh *et al.*, 2008) are used. First the case when all nodes are solar powered is considered and then results for the hybrid case are presented. All node batteries are fully charged prior to the deployment and bandwidth matrices are chosen randomly. In these particular results the bandwidth flows are assumed to be temporally variable with durations chosen uniformly and with the number of new bandwidth flows at each hour randomly chosen from a Poisson distribution. Bandwidth flow rates were taken to be normal and the sources and destinations were chosen uniformly. These parameters are varied to obtain different network energy loading values.

In Table 3.1 an example for a temporary deployment of 1 month (i.e., the entire month of February) is presented using solar insolation data for Toronto, Canada. The results consist of values for the total energy provisioning cost, for several different values of average normalized flow rate, which are expressed in average power consumption. Results for the SPRP Algorithm are compared to the cost bound derived in Section 3.3.2. As seen in Table 3.1 the bound is about 56% lower than the cost obtained by the SPRP Algorithm when the power load is 1 W on average. In addition it can be seen that as the average loading increases, the difference between the bound and SPRP decreases slightly until it reaches about 42% at an average load of 6 W. When the average loading is lower, the bound takes the energy state of the nodes into account and can re-route flows through longer routes that have more available energy (either a higher energy replenishment rate or more battery energy), but when the network becomes overloaded, this extra energy will not be sufficient. In this case re-routing bandwidth will not be helpful since all routes may be heavily energy constrained. These results are for a network where there are multiple shortest path routes, and SPRP is expected to have good performance.

Results for the hybrid network case are now shown in Table 3.2. In these results, the same system assumptions are made as in the all-solar case discussed previously except

Average Load (W)	SPRP (CAD)	Lower Bound (CAD)	Savings (%)
1	132	90	32
2	80	24	70
4	156	131	16
6	174	121	31

Table 3.2: Hybrid Network Resource Assignment Cost vs. Average Load

that half of the nodes are randomly chosen to be continuously powered. The node costs for Dijkstra's algorithm were set to $d_s = 1$ and $d_c = 0$. As seen in Table 3.2 the lower bound results in savings when compared to SPRP as high as 70% when the average load is 2 W. However, since various parameters are randomly chosen, the SPRP results vary considerably compared with the bound. More results will be introduced later in the chapter that will better explain the savings trend as the load increases. Again, it can be noted that these savings are for a mesh where there are a large number of shortest path routes, so SPRP is expected to perform well. It would be expected to have a larger difference between SPRP and the bound in random networks for these reasons.

Although the tightness of the bound is not known, the large differences that are found between it and the SPRP results suggests that there may be better practical resource allocation mechanisms. In the next section it will be shown that this is indeed the case, but in order to obtain this improvement, the provisioning mechanism must take into account the use of energy aware routing.

3.5 Energy Aware Resource Provisioning (EARP)

The SPRP Algorithm introduced in Section 3.4 is a relatively straightforward procedure. Unfortunately, this approach, which is motivated by conventional PV provisioning, cannot generate resource assignments that include the use of energy aware routing. Whenever the resource assignment changes, the resulting change in the energy states of the nodes may alter the route selection, which may then lead to a different resource assignment. To obtain a true optimum resource configuration in this case is exceedingly difficult. Unlike the bound derived in Equations 3.2 to 3.11, the routing must account for the energy states of the nodes in a causal fashion with respect to both future changes in the bandwidth load and solar insolation inputs. This is a difficult non-linear optimal control problem.

To address this problem a genetic algorithm approach is proposed to obtain resource assignments using causal energy aware routing. Genetic algorithms are well-suited for this type of multi-constraint problem especially since it includes a large non-convex search

space (Wong *et al.*, 1996). Genetic algorithms have been used in the past to size PV power systems (Xu *et al.*, 2005)(Shahirinia *et al.*, 2005) and have also been applied to certain energy aware routing problems (Sirikonda, 2007)(Ahn and Ramakrishna, 2002). In our case the genetic algorithm is used to choose a combination of battery capacities when the system is operated using a causal energy aware routing algorithm. If the network lives for the required design lifetime, then this solution is feasible, and the GA proceeds to consider other combinations.

3.5.1 Genetic Representation

A genetic algorithm (GA) is a search technique used to find exact or approximate solutions to optimization and search problems. This approach is a good choice for our problem since they can handle multi-objective functions and multi-constraint problems (Ko *et al.*, 1997). A GA can be briefly described as follows (Ko *et al.*, 1997). Each possible solution (chromosome) can be considered an *individual*. This individual is made up of a number of genes which are each represented using a string of integers, which in our case represent the maximum battery capacity for each node. Genes can change order from one generation to the next. Standard genetic algorithm manipulations, such as crossover and mutation, mix and recombine the genes of a parent population (mating pool) to form offspring for the next generation. Which offspring survive to the next generation is specified by a *fitness function*, $\mathcal{Y}$. The fitness function in our case will be the total cost of the network for a given set of $B_{max}(i)$. In this process of evolution (manipulation of genes), the fitter chromosomes will create a larger number of offspring, and thus have a higher chance of survival to subsequent generations. GAs repeat this cycle until they reach a desired termination criterion such as a given number of iterations or the variation of individuals between different generations, or a predefined fitness value.

A chromosome of the proposed GA consists of sequences of positive integers representing the battery capacity of each node. The length of the chromosome is the number of nodes in the network. The choice of the population size is a very important factor in the GA. Small populations execute quickly but they may not explore the entire search space. By experimenting, it was found that a population size that is equal to twice the size of the network (number of nodes) performs well for our problem.

Crossover is a genetic operator that combines (mates) two chromosomes (parents) to produce a new chromosome (offspring). The idea behind crossover is that the new chromosome may be better than both of the parents if it takes the best characteristics from each of the parents. Uniform crossover is chosen where the operator decides (with some probability) which parent will contribute each of the gene values in the offspring chromosomes (Marczyk, 2004). As mentioned above our chromosome represents the battery capacity of each node, so using single point crossover will take one half of the new chromosome from a parent and the other half from the other parent which will not work well in

our case. This is because the resource assignment is dependent on the location of the node in the network so if the routing is loading a part of the network more than another part, the single point operator may create an offspring that is infeasible. On the other hand, uniform crossover does the mating on the gene level so this will allow for more diversity and better exploration of the search space.

Selection is a genetic operator that chooses a chromosome from the current generation's population for inclusion in the next generation's population. Before making it into the next generation's population, selected chromosomes may undergo crossover and/or mutation (depending upon the probability of crossover and mutation) in which case the offspring chromosome(s) are actually the ones that make it into the next generation's population. Tournament selection is used because it tends to maintain diversity of the population (Marczyk, 2004).

Another parameter for the GA is the fitness function, $\mathcal{Y}$. Our fitness function will accept the chosen set of $B_{max}(i)$ as an input and report the cost of the network which is taken to be the summation of the battery capacities, i.e., the fitness function is given by

$$\mathcal{Y} = \sum_{i \in \mathcal{N}_s} B_{max}(i), \tag{3.15}$$

which is identical to the first term of the objective function defined in Equation 3.2. The GA search space will be restricted as a constraint based on the lifetime of the network while using energy aware routing. In this formulation, an energy-aware routing algorithm is used based on the use of Dijkstra's Algorithm with a node cost function given by

$$C(i,k) = \begin{cases} 0, & i \in \mathcal{N}_\infty \\ \frac{1}{\zeta^{B(i,k)/B_{max}(i)}\ \mathcal{P}(i)\ \mathcal{E}(i,k)}, & i \in \mathcal{N}_s \end{cases} \tag{3.16}$$

where ζ is a large constant. Although any causal energy aware routing can be used in this procedure, Equation 3.16 was chosen because it incorporates both the node energy state and the solar insolation renewal rate. In (Zeng *et al.*, 2009) this link cost metric was found to produce good results for networks operating with renewable energy sources. Setting $C(i,k)$ to zero for continuously powered mesh nodes makes the routing algorithm strongly prefer these nodes during route selection. This will tend to off-load the solar powered nodes, resulting in cost improvements since the cost of continuously powered nodes is independent of bandwidth loading.

Each iteration of the EARP algorithm includes a recursive computation of the network energy flow over the input sample functions, which is summarized in Algorithm 2. At every Δ increment k, for each Node i, the cost applied to links associated with that node using Equation 3.16 is computed. Dijkstra's Algorithm is then used to assign all of the input bandwidth flows. Following this, the energy loading is calculated for each node using

Algorithm 2 EARP GA Flow Procedure

for all $k_{min} \leq k \leq k_{max}$ **do**
  for all $1 \leq i \leq N$ **do**
    Compute $C(i,k)$ from Equation 3.16.
  end for
  Use Dijkstra's Algorithm to assign bandwidth flows at time $k\Delta$.
  for all $1 \leq i \leq N$ **do**
    Calculate the Node i energy load using Equation 3.14.
    Update $B(i,k)$ using Equation 3.1.
  end for
end for

Equation 3.14, and the battery states are updated using Equation 3.1.

3.6 Simulation Model and Results

The performance of the proposed resource assignment algorithms has been extensively characterized using both fixed and variable bandwidth usage profiles in various geographic locations. Since both result in similar conclusions, in this section results that are typical of the variable BUP case are presented. Random uniform network topologies are considered in simulations where the nodes are distributed uniformly at random in a square area and as before radio power consumption parameters which are consistent with typical IEEE 802.11 values (Farbod and Todd, 2006) are assumed. In the following the results for 2 different scenarios are presented, i.e., the all-solar and hybrid network cases. In both of these scenarios 3 different sets of simulations are examined, focusing on the effect of the network topology, weather conditions (winter versus summer) and average network load. All of the results presented are averaged over 50 runs. All solar powered nodes have a full initial battery state prior to the deployment. The number of bandwidth flows available at each hour and the bandwidth flow rates were chosen randomly as in Section 3.4.1. In all of our experiments the bandwidth flows are assumed to be temporally variable and the duration of each bandwidth flow are chosen randomly as before. Also, as in Section 3.4.1 the sources and destinations are chosen randomly. The genetic algorithm toolbox in Matlab is used, and Table 3.3 gives the default parameters that are used.

Parameter	Value
p: Population size	20
η: crossover rate	0.75
γ: mutation rate	0.12
max iterations	10
variation stop iterations	4
ϵ stopping threshold	1×10^{-4}

Table 3.3: GA Parameters

3.6.1 Solar Powered Network Examples

Using the proposed energy aware resource assignment methodology many experiments have been done which show the reductions in the costs of the assigned battery capacities that are possible. Table 3.4 finds the resource assignment for rectangular mesh networks with different sizes. The network lifetime is constant in most of the experiments and is assumed to be 1 month and Table 3.4 shows the results for 20 different networks. As shown in the table the EARP resource assignment gives a much lower cost than using SPRP. By comparing EARP and SPRP, it can be noted that for a 3×3 network, the EARP assignments save roughly 28% from the total cost of the network. Moreover, the savings for different rectangular networks are almost the same, i.e., it ranges from 15% to 31%. However, if rectangular network results are compared with those of randomly generated networks the savings in random networks are much higher, e.g., 49% savings in the random network case and 31% for rectangular mesh networks when there are 25 nodes. This is due to the fact that in random networks there are fewer shortest paths, which leads to larger EARP improvements. Note that in the results for the random networks case, the values plotted are averaged over all the generated networks, including those for the bound. It can be seen that the difference between the bound and SPRP is 93% for the 5×5 network and 140% for the 25 node random networks. This suggests that EARP has better relative performance in random networks than in rectangular grids. In addition to that in the 3×4 and 4×3 networks the difference between SPRP and EARP is the same. Furthermore, the difference between EARP and the bound ranges from 47% to 90% which is a large improvement compared to the difference between SPRP and the bound that ranges from 92% to 140%. As expected, the bound is not particularly tight since it uses future solar insolation and bandwidth inputs and is therefore not causal. However, it does provide a useful gauge for how the algorithms are performing.

In the next set of figures, the battery costs of 15 node random networks are compared when using EARP and SPRP. The experiments are conducted for deployment windows which occur during the winter and summer, in Toronto, Canada using the same system

Network Size	SPRP	EARP	Lower Bound	Savings (%)		
				EARP/ SPRP	Bound/ EARP	Bound/ SPRP
3 × 3	219	172	97	28	77	126
4 × 4	513	448	264	15	70	94
5 × 5	600	458	311	31	47	93
4 × 3	326	284	170	15	67	92
3 × 4	341	297	156	15	90	119
25 node random	510	352	213	49	65	140

Table 3.4: Cost in CAD vs. Network Size for SPRP and EARP Resource Provisioning

assumptions as before.

Figure 3.2 shows the results for the deployment periods during the winter. The horizontal axis spans a time which starts at the first of December and ends at the end of March. The experiments are run over 100 different random networks, and as can be seen in the figure, EARP has a significantly lower cost than SPRP. It can be noted that there is a savings of roughly 30% in the battery cost when the lifetime is almost 3 months. Moreover, the cost slope increase is larger at the left of the figure. This is because as the lifetime increases the network begins to enter the summer where the main cost of the networks is the cost of the solar panels and not the batteries. For this reason the battery cost remains fairly constant during the summer months. Moreover, the difference between EARP and SPRP increases as the lifetime increases. This is due to the fact that for longer lifetimes, EARP can save more by using longer routes that already have resources rather than by adding new resources for shorter routes as SPRP tends to do.

Figure 3.3 shows similar results for summer time deployment periods. The horizontal axis spans a time which starts at the first of July and ends at the end of October. In this figure, the cost of the network increases for the first couple of months which accommodates the extra costs needed for longer lifetime, but then the cost becomes almost constant. This is because the network is using renewable energy and as it moves towards the winter, the costs of the networks begin to increase again. However, it can be seen that even in the summer, EARP provides significant savings when compared to SPRP, for example, EARP achieves savings of about 60% when the network lifetime is 3 months. In addition to this, for longer lifetimes, more savings from EARP are gained when compared to shorter lifetimes.

In Figure 3.4 the effects of relative network cost for SPRP, EARP and the bound are examined as the average energy loading of the network is varied. Simulations are run on 20 nodes random networks for 1 month. It can be noted that when the network is overloaded EARP provides more savings. This is due to the fact that EARP will reuse the nodes when

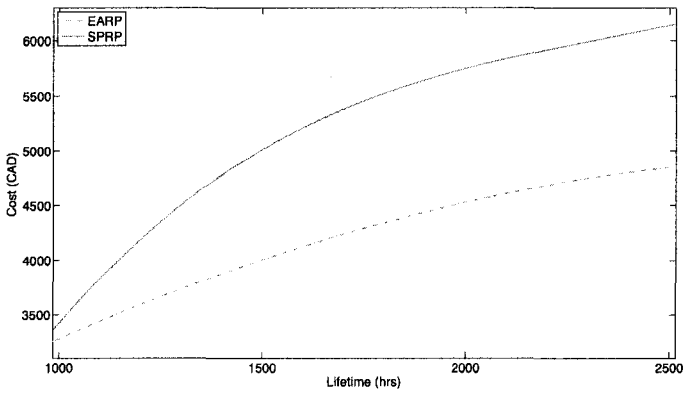

Figure 3.2: Battery cost vs. Lifetime for Different Resource Assignment Algorithms (Winter Months)

the network is overloading leading to more savings. This is different from the rectangular mesh results that had been discussed previously. In a rectangular mesh the savings tend to decrease as the load increases because all routes are shortest path routes. In this case the best way to save energy is to uniformly distribute the load on all nodes so when the load increases energy awareness doesn't have much room for improvement. On the other hand, in random networks not all routes are shortest path, so as the load increases shortest path routing will perform poorly by over provisioning nodes on the shortest path routes where energy aware routing may choose longer routes. This leads to the enhanced performance of energy aware routing in overloaded networks. It can be seen that when the average load is 4 W EARP has 113% savings. Moreover, the increase in the network cost is almost linear with the load up to a certain point. In addition to that, EARP leads to a cost increase of around 25% when compared to the bound and this is because the bound assumes a perfect knowledge of bandwidth flows and solar insolation so it can save more energy using the optimum routes to route the flows.

3.6.2 Hybrid Network Examples

In this section the performance of the resource assignment schemes for hybrid networks is compared. The same simulation setup and parameters are used as in Section 3.6.1 except that in all of the examples half of the nodes are randomly assigned to be continuously powered.

In the first set of results the resource assignment for rectangular mesh networks with

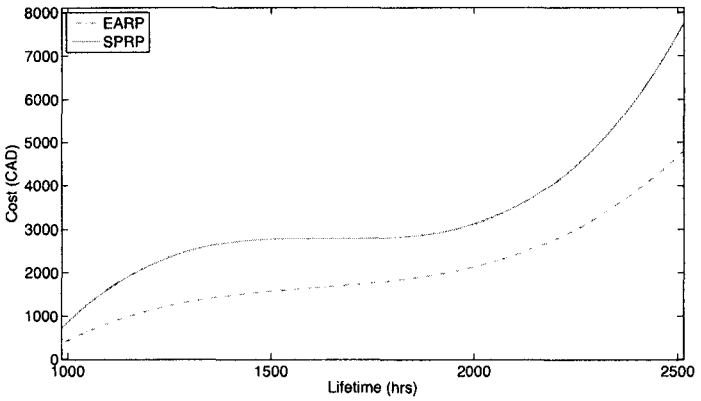

Figure 3.3: Battery cost vs. Lifetime for Different Resource Assignment Algorithms (Summer Months)

different sizes is found. The network lifetime is the same for all the experiments and is assumed to be 1 month. These results are presented in Table 3.5 where it can be seen that the EARP resource assignment gives a much lower cost. In comparing the two algorithms, it can be noted that for a 4×3 network, the EARP assignments save roughly 53% from the total network cost. Moreover, the hybrid case has more savings than the all solar case (for a 4×3 network the solar case has 15% savings compared to 53% in the hybrid case). This is because EARP is better able to take advantage of the continuously powered nodes. For the all solar case that, random networks have more savings than rectangular mesh networks (i.e.,130% saving for the 5×5 grid compared to 234% for the 25 node random networks). In grid networks there are many shortest paths so energy aware routing is less able to improve over SPRP in certain situations. Furthermore, the difference between SPRP and the bound is much more in the hybrid case when compared to the all solar case (200% for the 4×3 network compared to 92% for the same network in the all solar case). The difference between SPRP and the bound is almost triple the difference between EARP and the bound which shows the large savings obtained from considering energy aware provisioning.

The next set of figures compares the battery cost of 15 node random networks when using EARP and SPRP. As before, the experiments are conducted for deployment windows which occur during the winter and summer, in Toronto, Canada. Figure 3.5 shows the results for the deployment periods during the winter. The horizontal axis spans a time which starts at the first of December and ends at the end of March. The experiment is run over 100 different random networks. As can be seen in the figure, EARP has a significantly lower cost. It can be noted that there is a savings of 73% in the battery cost when the lifetime

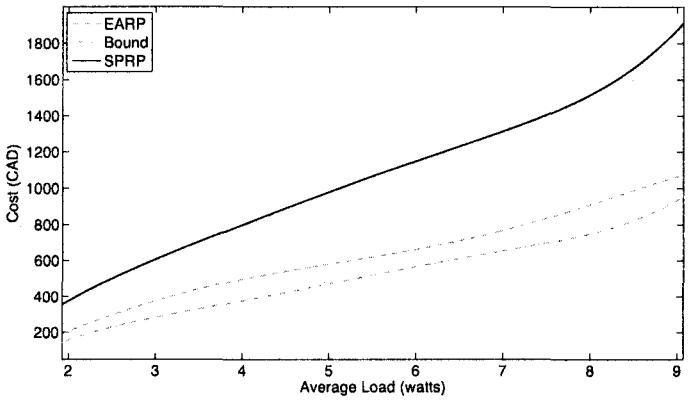

Figure 3.4: Cost vs. load for Different Resource Assignment Algorithms (Winter Months)

is almost 2 months. Moreover, the same behavior in the slope and the cost differences is seen as in the all solar case.

Figure 3.6 shows the results for the deployment periods during the summer. The horizontal axis spans a time which starts at the first of July and ends at the end of October. In this figure the same behavior as in the all solar case is seen. When the network lifetime is 3 months EARP saves 84% of the provisioning cost. In addition, it can be noted that again for longer lifetimes EARP has more savings compared to SPRP. The continuously powered nodes do not decrease the cost of the network during summer as is the case during the winter. This is again because the summer has high solar insulation so the recharge rate of most of the nodes is high, making them as good as continuously powered nodes.

In Figure 3.7 the cost versus network loading is plotted for SPRP, EARP and the bound. The results are run on 25 node networks for 1 month. The difference in this case between SPRP and EARP is about 30% and between EARP and the bound is about 20%.

3.7 Discussion

3.7.1 Provisioning Resiliency

The results presented in Sections 3.6.1 and 3.6.2 clearly show the cost advantages that energy aware provisioning can provide. These reductions result from a decrease in total network energy resources compared with that obtained using the SPRP Algorithm. An issue which may arise is that compared to SPRP, in some cases the EARP-provisioned network may be less able to accommodate bandwidth flows which differ from that for

Network Size	SPRP	EARP	Lower Bound	Savings (%)		
				EARP/ SPRP	Bound/ EARP	Bound/ SPRP
3×3	118	83	44	42	89	168
4×4	177	144	91	23	58	95
5×5	216	94	39	130	141	454
4×3	180	118	60	53	97	200
3×4	192	128	87	50	47	121
25 node random	204	61	23	234	165	787

Table 3.5: Resource Assignment Cost vs. Network Size

which the network was provisioned. In this section some results will be shown which illustrate that this can be the case.

In the presented results 15-node random networks were used. After the initial resource assignment is done, the network is subject to an overload bandwidth flow matrix. Using this input and the resource assignments the network is run for the desired network lifetime. The network that was designed using SPRP is tested using shortest path routing while the network that was designed using EARP is tested using energy aware routing. It is expected that the networks will not operate outage-free for the full lifetime duration since the system is now under-provisioned. To characterize this the *competitive ratio* is calculated for each algorithm as its lifetime normalized to the design lifetime, i.e.,

$$\text{Competitive Ratio (CR)} = \frac{\text{Actual lifetime}}{\mathcal{T}_{\mathcal{L}}}. \tag{3.17}$$

The actual lifetime is determined when a node outage prevents one or more flows from reaching their destination.

In Figure 3.8 the competitive ratios of SPRP and EARP are plotted versus the average bandwidth overload. As seen in the figure, the competitive ratio of SPRP exceeds that of EARP because the SPRP network is over-provisioned and is better able to handle unforeseen loading. However, as the load increases, the performance of SPRP and EARP become very similar because the extra resources cannot support the additional bandwidth load and the network runs into outage. A similar result is shown in Figure 3.9 which makes the same comparisons for an all solar network example. In this case the differences are much more significant when the average overload is 1.5 to 3 times the design values. In (Badawy *et al.*, 2008) this effect was also characterized using different shortest-path and energy-aware provisioning and routing combinations. This thesis also found that the differences in competitive ratio are much smaller in rectangular mesh networks compared to the random

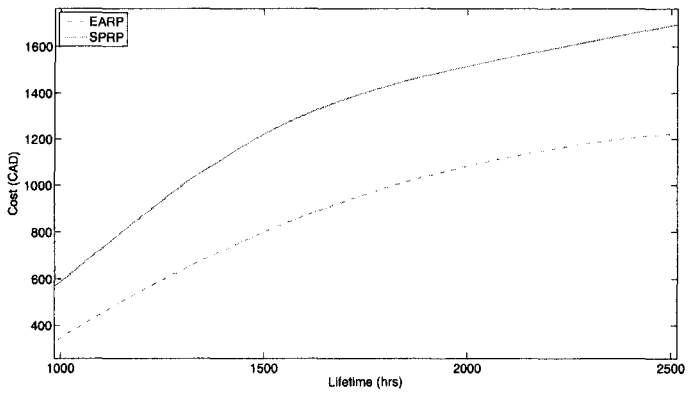

Figure 3.5: Battery cost vs. Lifetime for Different Resource Assignment Algorithms (Winter Months) for Hybrid Mesh Networks

network case. Similar results show that when bandwidth flows significantly de-correlate compared with the design profile, a more accurate algorithm such as EARP may be less able to accommodate unforeseen bandwidth conditions.

These results confirm our intuition that in some cases a more precisely provisioned network may be less able to adapt to unforeseen bandwidth scenarios. This should be taken into account when defining the bandwidth profile that is used in the design process. If network usage parameters can be predicted well in advance, then significant cost savings can be obtained by energy-aware provisioning combined with small bandwidth margins. If bandwidth differs significantly from that used in the provisioning, then in practical deployments this may lead to higher bandwidth deficits when an outage control algorithm is used (Sayegh, 2008). This may be perfectly acceptable in many applications.

3.7.2 Algorithm Complexity

The SPRP Algorithm uses Dijkstra's Algorithm in order to determine network bandwidth flows and this is repeated for each Δ deployment time interval. For this reason, the time complexity of finding the loading for each node can be shown to be polynomial. Following this, the node provisioning process occurs which consists of N independent 1-dimensional minimizations through the convex battery capacity space. Each search step involves the evaluation of the energy flow equation for the deployment time period in the worst-case. Since this line search is convex, it can be done with an approximate linear convergence, which is very fast in practice. In our experience this entire process can be achieved very

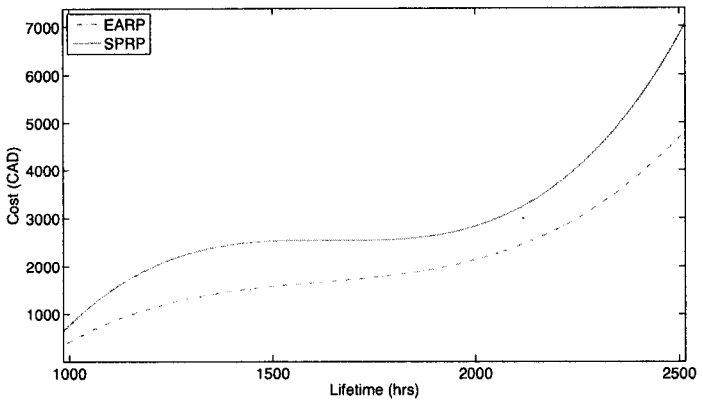

Figure 3.6: Battery cost vs. Lifetime for Different Resource Assignment Algorithms (Summer Months) for Hybrid Mesh Networks

quickly and there is no practical complexity issue.

Genetic algorithm complexity is much more difficult to generalize because the time complexity is known to be related to the characteristics of the problem domain (Rawlins, 1991). Unlike many problems, fortunately our fitness function is very simple and can be computed almost instantly. It has been found during this work that as the number of nodes or hours increase, the GA algorithm run-time may increase considerably. In the worst-case for the results presented in this chapter, it took up to 5 days to provision a 15-node network using a 3000 hour time sample function. It has also been noticed that rectangular mesh networks take significantly longer to process than the random networks that were generated. This is due to their higher route diversity. Fortunately our problem is an off-line one where the provisioning is done long in advance of the actual network deployment, and thus this level of complexity is acceptable for this application. This is clearly the case for metro-area WLAN mesh network deployments since typically hop counts are limited to three or four, so that capacity latencies and link sharing are restricted.

3.8 Conclusions

In this chapter the problem of solar panel and battery resource assignment in solar powered WLAN mesh networks has been studied. The objective of this type of provisioning is to find an assignment which ensures outage-free operation based on historical solar insolation traces and an input bandwidth load profile for the network. This problem has been studied from a network viewpoint rather than from that of a single node as is often the case in the

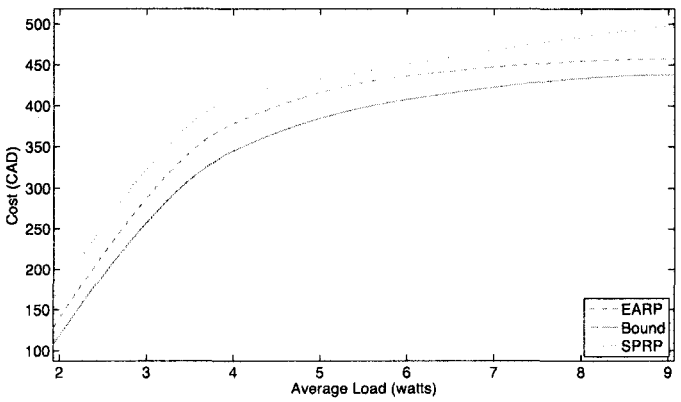

Figure 3.7: Cost vs. load for Different Resource Assignment Algorithms for Hybrid Mesh Networks

literature.

A flow-based provisioning procedure (SPRP) was first introduced which is motivated by conventional single system photo-voltaic provisioning approaches. This method is based on deriving temporal shortest path routes, and then simulating each node independently using its energy flow equation and a power dissipation model. A linear programming optimization was formulated which finds a lower bound on the resource assignment problem for a given set of inputs. The cost differences between the bound and SPRP motivated the development of a new methodology based on the use of a genetic algorithm using energy aware routing (EARP). The case has also been considered where some network nodes are designated as having continuous power connections.

Extensive simulations have been done which evaluate the proposed methodologies using different network topologies and using different solar insolation inputs. Some representative examples of these results were presented. The results have shown that as the route diversity in the network decreases, more savings can be obtained from an energy aware resource provisioning. This was shown for example, when 25 node random networks were compared to 5×5 mesh networks and 45% savings were found for the random network compared to 30% savings for the mesh network. Moreover, it has been shown that for 15 node random networks allow savings of 30% for winter time compared to 60% in the summer. This is because in summer there is much higher solar energy and energy aware routing more effectively uses routes that can harvest this energy. In addition, it has been shown that for networks that have a variety of different path lengths, benefits from energy aware routing increases as the average load on the network increases. A 113% reduction

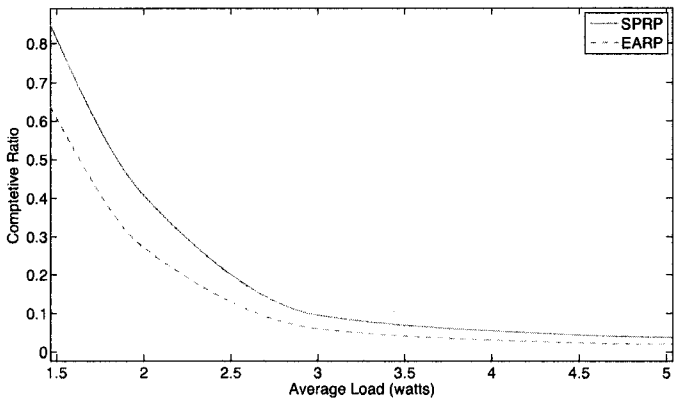

Figure 3.8: Competitive Ratio vs. Load Factor for SPRP and EARP (Hybrid Networks)

in the network cost is achieved when the average load is 6W compared to 103% when the average load is 4. For networks with a high number of shortest path routes this is not the case. On the contrary, the savings decrease as the average load increases. When the network is loaded, energy aware routing is not able to use alternative routes to save energy since all routes tend to be used and there is less free energy. From a network resiliency viewpoint, it can be seen that the competitive ratio of EARP is lower than that of SPRP. This trend decreases when the network becomes heavily overloaded in the cases that were considered. In conclusion, significant cost savings can be achieved by using energy aware routing when provisioning the network when compared to using SPRP. All these savings are increased substantially when hybrid networks with a mixture of solar and continuously powered nodes are considered.

In the next chapter the problem of fair bandwidth control in solar powered wireless mesh networks is addressed. A mathematical formulation for this fair bandwidth control is given which is used to obtain an upper bound on the admitted flows. The problem is formulated using a utility fairness function and max/min fairness is chosen for the represented results. A causal bandwidth control algorithm that is motivated by the optimization framework is presented. The algorithm uses solar insolation prediction based on access to on-line historical weather data. Results show that the proposed algorithm eliminates node outage and performs very well compared to the optimum bandwidth control bound.

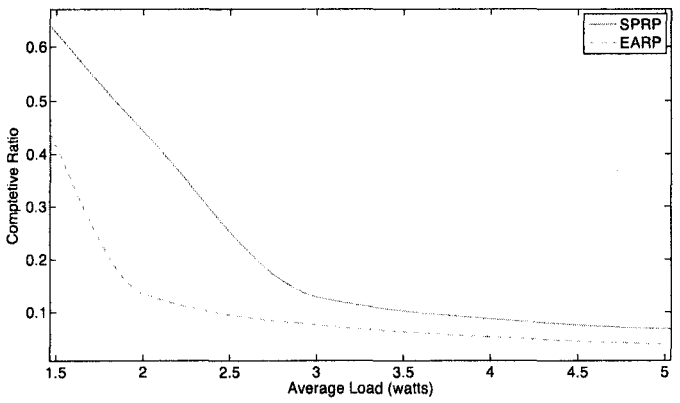

Figure 3.9: Competitive Ratio vs. Load Factor for SPRP and EARP Algorithms (All Solar Networks)

Chapter 4

Fair Bandwidth Control in Solar Powered Wireless Mesh Networks

4.1 Introduction

As shown in the previous chapter, the resource allocation process for solar powered wireless mesh networks involves assigning a solar panel and battery capacity to each mesh node. Once the network is deployed however, its performance may become unreliable in cases when the actual bandwidth usage profile deviates significantly from the design phase workload. If no bandwidth flow control is in place, the nodes may experience outage, resulting in an in-operable network. To prevent this from happening, the nodes must flow control input traffic in such a way that outage is prevented and yet the best possible performance is obtained. This control action will result in a bandwidth deficit and should be applied in a manner that is temporally fair.

In this chapter a mechanism for controlling the bandwidth flows in these types of networks is proposed. The problem is first formulated as an optimization using a convex utility fairness objective function. Using this optimization, a non-causal max/min fairness bound is generated based on the knowledge of future solar insolation data and a bandwidth usage profile. A flow control algorithm is then presented that is motivated by the optimization framework which uses solar insolation prediction based on access to on-line historical weather data. The results show that the proposed algorithm eliminates node outage and performs very well compared to the optimum flow control bound for a variety of network scenarios.

4.2 Background

Previous work on flow fairness has considered it at different protocol layers. Fairness at the MAC layer deals with per node fairness, but does not ensure network layer fairness as discussed in (Hsieh and Sivakumar, 2001). Network layer fairness is concerned with per flow fairness, so that nodes having higher numbers of flows can be given more packet forwarding bandwidth. In (Shagdar and Zhang, 2005) a scheme was proposed that improves the per flow MAC and link layer flow fairness. The link layer fairness is achieved by allowing the link layer to send packets to the MAC layer using an RR (Round Robin) scheduler. The MAC layer fairness is achieved by allowing nodes to send multiple packets from different flows when they acquire channel access. The proposed scheme requires minor modifications to the original IEEE 802.11 media access control protocol, and the authors show that it improves the flow fairness and overall performance of the network. However, this work does not take end-to-end flows into consideration.

The work in (Retvari *et al.*, 2007) formulates an optimization problem to solve the per flow fairness problem independently of the routing algorithm. Using a polyhedral description, it was shown that there always exists a unique routing-independent max/min fair throughput allocation in a regular network, which can be obtained by an extension to the water-filling algorithm. An issue with this approach is that it requires that the throughput polytope be available in advance, which requires a substantial computational effort, and may be intractable for large networks. Neely et al. considered an optimal control for general networks with both wireless and wireline components and with time varying channels (Neely *et al.*, 2008). The problem was decoupled into separate algorithms for flow control, routing, and resource allocation. The combined strategy was shown to yield data rates that are arbitrarily close to the optimal operating point achieved when all network controllers are coordinated and have perfect knowledge of future events. In this work the networks do not operate under energy constraints.

Reference (Johansson and Xiao, 2004) considers the problem of finding the jointly optimal end-to-end communication rates, routing, power allocation and transmission scheduling for wireless ad-hoc networks with the objective of maximizing the throughput while considering end to end rate fairness. The authors formulate their cross-layer design problem as a nonlinear optimization problem. Moreover, they develop a specialized solution method based on Lagrange duality and column generation and demonstrated the approach on several examples. Chen et al. (Chen and Zhang, 2006) propose an end to end aggregate fairness model, for wireless sensor networks. They then propose a distributed aggregate fairness algorithm (AFA) that implements the model. AFA is a localized algorithm that doesn't maintain any per-flow information or global state. Each sensor performs localized operations, yet the collective outcome ensures a fair access to the network bandwidth. In addition, AFA automatically adjusts each sensor forwarding rate to avoid packet drops due to congestion. The simulation results demonstrate that the proposed algorithm effectively

improves end-to-end fairness.

In (Zhu *et al.*, 2006) the tradeoff between network lifetime maximization and fair rate allocation is studied in sensor networks with multi-path routing. The problem is formulated as a constrained maximization with a single weighted objective that is the summation of both objectives. An iterative partially distributed algorithm is presented. The presented algorithm works well for small problems but it is not efficient for large scale networks.

This chapter considers bandwidth control for renewable energy wireless mesh networks, which to our knowledge has not been previously considered in the literature.

4.3 Fair Bandwidth Control Problem Statement

Fair bandwidth control involves the admission of a portion of the requested bandwidth $A(b,k)$ for each bandwidth flow b at each time instance k, so that network outage is prevented. This is done using estimated future solar insolation traces for the desired geographic deployment location, i.e., using an estimation of $\mathcal{E}(i,k)$ derived from recorded historical data.[1] The problem is as follows.

- As in Section 3.3.1, the mesh network consists of N nodes modeled as a *directed graph* where each mesh node represents a vertex and two nodes can have an edge (i.e., a link) between them if they are within communication range. Each node is identified by an index in the set $\mathcal{N} = (1, 2, \ldots, N)$ and each edge is defined by an ordered pair (i,j) where $i,j \in \mathcal{N}$ are the transmitting and receiving nodes, respectively. The set of all edges is denoted by E. Each node has an assigned solar panel size $P(i)$ and battery capacity $B_{max}(i)$ where $i \in \mathcal{N}$. Traffic is relayed in a multi-hop fashion and a path from source to destination consists of one or more adjacent edges.

- Sample functions consisting of a bandwidth usage profile (BUP) and estimated solar insolation input trace are given for a contiguous deployment time period, $\mathcal{T}_{\mathcal{L}}$. The usage profile consists of a multi-commodity bandwidth usage matrix $\mathcal{M} = [m_{sd}(k)]$, where $m_{sd}(k) \geq 0$ indicates the aggregate bandwidth requirement from Node s to Node d during time period $((k-1)\Delta,\ k\Delta)$. The estimated solar insolation sample function consists of an input trace over the same time period whose values at Node i are given by $\mathcal{E}_{SIM}(i,k)$.

  The deployment time period is given by $\mathcal{T}_{\mathcal{L}} = (k_{min}\Delta, k_{max}\Delta)$ where k runs over the set $\mathcal{K} = (k_{min}, k_{min}+1, \ldots, k_{max})$.

[1] For the USA, this type of data is available from the National Renewable Energy Laboratory (NREL), U.S. Department of Energy, and for Canada it can be obtained from The Meteorological Service of Canada. These databases include solar insolation samples that span several decades of continuously collected measurements for hundreds of different geographic locations. Temperature samples are also included with the solar insolation traces.

- The objective is to admit a portion $A(b,k)$ for each bandwidth flow b at each time instance k in a spatially and temporally fair manner when Equation 3.1 is applied such that $B(i,k) > B_{outage}(i)$ for $k \in \mathcal{K}$ and $i \in \mathcal{N}$.

In order to generate practical bandwidth control algorithms, the sample function values must be provided to the system in a causal fashion so that future values are not known to the system as Equation 3.1 is evaluated.

In order to investigate the quality of various bandwidth control mechanisms, in the next section an upper bound is derived on the maximum admitted usage profile. This bound is compared with the FFRBC Algorithm introduced in Section 4.5.1 and FVRBC Algorithm introduced in Section 4.5.2.

4.4 Fair Bandwidth Control Bounds

Given solar insolation data and a bandwidth usage profile, upper bounds are computed on the optimum admitted input flows, given that the solar panel sizes and battery capacities are pre-determined. The bound is obtained by formulating the problem as a constrained optimization, and by incorporating all future solar insolation inputs. This result gives a non-causal bound on the bandwidth control performance of the network for any realizable (causal) algorithm that operates using the same inputs. This bound is compared with causal fairness algorithms that are considered later in the chapter.

The objective is a fair admission of bandwidth flows subject to satisfying the routing and battery constraints, i.e., an Edge (i,j) can only be assigned to a bandwidth flow when the energy levels at Nodes i and j are above $B_{outage}(i)$. The bound applies to bandwidth usage profiles which contain a mixture of high priority and low priority bandwidth requests. The set of high priority bandwidth flows is defined as $\mathcal{M}_h$, and those with low priority as $\mathcal{M}_l$, where $\mathcal{M} = \mathcal{M}_h + \mathcal{M}_l$. High priority bandwidth flows have to be fully admitted (i.e., $A(b,k) = 1 \quad \forall b \in \mathcal{M}_h$). To achieve the objective, a utility fairness function is used, $\mathcal{U}(b,k)$, as discussed in (Boudec, 2008) and defined below. The optimization problem can then be written as follows. A discussion of the various terms is given afterwards.

$$maximize \sum_{b\in\mathcal{M}}\sum_{k\in\mathcal{K}} \mathcal{U}(b,k) - \lambda_1 \sum_{i\in\mathcal{N}}\sum_{k\in\mathcal{K}} L(i,k)$$

subject to the following constraints.

$$0 \leq f_{ij}(k) \leq 1 \tag{4.1}$$

for all $(i,j) \in E, k \in \mathcal{K}$, and,

$$A(b,k) = \begin{cases} 1, & b \in \mathcal{M}_h \\ \leq 1, & \text{otherwise.} \end{cases} \tag{4.2}$$

$$A(b,k) \geq 0 \tag{4.3}$$

for all $b \in \mathcal{M}$, $k \in \mathcal{K}$ and,

$$\sum_{(i,l)\in E} f_{il}(k) + \sum_{b\in\mathcal{M}} \sum_{d\in\mathcal{N}} A(b,k) m_{id}(k) = \sum_{(h,i)\in E} f_{hi}(k) + \sum_{b\in\mathcal{M}} \sum_{s\in\mathcal{N}} A(b,k) m_{si}(k) \tag{4.4}$$

for all $i \in \mathcal{N}$ and $k \in \mathcal{K}$.

$$B(i,k) = \min\{\max[B(i,k-1) + \mathcal{P}(i)\,\mathcal{E}(i,k) - L(i,k), B_{outage}(i)], B_{max}(i)\} \tag{4.5}$$

for all $i \in \mathcal{N}, k \in \mathcal{K}$.

$$\begin{aligned} L(i,k) = (&\sum_{(i,l)\in E} R f_{il}(k) + \sum_{(i,l)\in E} T\alpha f_{il}(k) + \sum_{(h,i)\in E} T f_{hi}(k) \\ &+ \sum_{(h,i)\in E} R\alpha f_{hi}(k) + \sum_{(i,l)\in E} S(1 - f_{il}(k) - \alpha f_{il}(k)) \\ &+ \sum_{(h,i)\in E} S(1 - f_{hi}(k) - \alpha f_{hi}(k)))\Delta \quad \forall i \in \mathcal{N}, k \in \mathcal{K}. \end{aligned} \tag{4.6}$$

$f_{ij}(k)$ in Equation (4.1) is the decision variable, and $A(b,k)$ is the portion of flow b admitted to the network at time k. If $f_{ij}(k) \geq 0$ then link (i,j) is on the available path at time instance k, otherwise $f_{ij}(k) = 0$. Constraint (4.1) is the link capacity constraint and Constraints (4.2) and (4.3) are the upper and lower bounds for $A(b,k)$. Constraint (4.4) ensures flow continuity and Equation (4.5) is the battery energy flow recursion. Constraint (4.6) is the total load on each node. The second term in Line 1 of Equation (4.6) and the first term in Line 2 are the energies associated with ACKs and other associated reverse-link flows, while the second term in Line 2 and Line 3 computes the energy consumed in power save mode. The utility fairness function is given by

$$\mathcal{U}(b,k) = 1 - \frac{1}{A(b,k)^{\beta}}, \tag{4.7}$$

where $\beta \geq 0$ is a design parameter, called the fairness index. Using (4.7), a large range of

fair flow control objectives can be modeled. The max/min fairness objective is chosen for this problem so the fairness index is chosen as $\beta \rightarrow \infty$, as discussed in (Boudec, 2008). The second term in the objective function minimizes the load on each node and is added to ensure that the optimizer will choose loop free routes.

The objective function and the constraints in the above optimization problem are all convex except for Constraint (4.5). However, this problem can be simplified to a convex optimization problem by introducing a new variable, $s(i,k)$, that was introduced in the previous chapter. Therefore, Constraint (4.5) can be replaced by

$$B_{outage}(i) \leq B(i,k) \leq B_{max}(i), \tag{4.8}$$

for all $i \in \mathcal{N}, k \in \mathcal{K}$, and,

$$B(i,k) + s(i,k) = B(i,k-1) + \mathcal{P}(i)\,\mathcal{E}(i,k) - L(i,k). \tag{4.9}$$

Constraint (4.8) sets lower and upper bounds for the energy levels in the batteries. Constraint (4.9) is the battery constraint that captures energy replenishment. The value of s should be minimized for all cases except when the non-linear constraint is active. Therefore, the objective function can be re-formulated as follows,

$$maximize \sum_{b\in\mathcal{M}}\sum_{k\in\mathcal{K}} \mathcal{U}(b,k) - \lambda_1 \sum_{i\in\mathcal{N}}\sum_{k\in\mathcal{K}} L(i,k) - \lambda_2 \sum_{k\in\mathcal{K}}\sum_{i\in\mathcal{N}} s(i,k), \tag{4.10}$$

where λ_1 and λ_2 are control factors that are set so as to not interfere with the operation of the original objective.

The above development finds a bound on the maximum admitted portion of each flow, and will in general admit different portions for each flow. These upper bounds are not necessarily achievable since they use optimal non-causal routing and assume perfect knowledge of future solar insolation. They do, however, provide an important basis for comparison with real flow control algorithms. This is done in Section 4.6. We first introduce some fair bandwidth control algorithms.

4.5 Fair Bandwidth Control Algorithms

In this section, a fair bandwidth control methodology is presented using causal routing algorithms. Two bandwidth control cases are considered. The first is Fair Fixed Rate Bandwidth Control (FFRBC), where all input traffic flows have a fixed request rate throughout the entire network lifetime. The second is Fair Variable Rate Bandwidth Control (FVRBC), where traffic flows may have variable rates during the network lifetime. The FFRBC case simplifies the flow control procedure so we will consider it first.

4.5.1 Fair Fixed Rate Bandwidth Control (FFRBC)

In this case a fixed bandwidth usage profile is admitted while using energy aware routing, taking into account that the solar insolation for the network lifetime is unknown, but whose statistical history is available. The bandwidth control algorithm chooses the portion of admitted bandwidth taking into account the energy state of the batteries. At first the solar insolation data is divided into two sets, one used for historical solar information data and the other is used for actual solar insolation input to the system. The proposed algorithm assumes that resource assignment has already been done as described in Chapter 3, and that the network is in operation. For a given deployment time window, $\mathcal{T}_{\mathcal{L}}$, the algorithm examines the requested bandwidth flows at every Δ interval, k, and runs the optimizer discussed in Section 4.4 for the remaining network lifetime, $\mathcal{T}_{\mathcal{L}}-k$. Since the solar insolation for the remaining network lifetime is unknown, an estimate based on the same deployment window, $\mathcal{T}_{\mathcal{L}}$, over the available set of historical solar insolation data is used. The mean solar insolation data used in the optimizer is calculated using

$$\mathcal{E}_{SIM}(i,k) = \mu_{\mathcal{E}(i,k)} + \gamma \cdot \sigma_{\mathcal{E}(i,k)} \tag{4.11}$$

for all $k \in \mathcal{K}$, $i \in \mathcal{N}$, where $\mu_{\mathcal{E}(i,k)}$ is the mean solar insolation over the 20 years of available solar insolation records, and $\sigma_{\mathcal{E}(i,k)}$ is the solar insolation sample standard deviation over the same period. The sensitivity factor, γ, is set to ensure outage free operation. Taking the output of the optimizer (from Equation 4.10), the algorithm admits a portion of each bandwidth request and routes the bandwidth flows using the optimal routing. Using these admitted bandwidth flows and routes, the algorithm calculates the load on each node. Then using the actual solar insolation data the algorithm updates the energy level at each battery using Equation 4.9. The algorithm continues this operation for the desired network lifetime, adjusting the admitted bandwidth portions every hour according to the actual solar insolation data. Since the bandwidth usage profile is fixed, the admitted bandwidth requests will only change according to changes in the solar insolation input.

4.5.2 Fair Variable Rate Bandwidth Control (FVRBC)

In this section a time varying bandwidth usage profile is admitted while using energy aware routing. The main difference between FVRBC and FFRBC is that at every Δ interval, k, the algorithm assumes that the traffic flows for the remaining lifetime are the same as in the previous hour. Using the assumed bandwidth usage profile, the algorithm runs the optimizer introduced previously. Taking the output of the optimizer (i.e., Equation 4.10), the algorithm calculates the load and updates the battery energy level at each node. Since the optimizer is using a different bandwidth usage profile and solar insolation data than the actual inputs, it is expected that its performance will be worse than that of FFRBC, where the bandwidth usage profile is fixed.

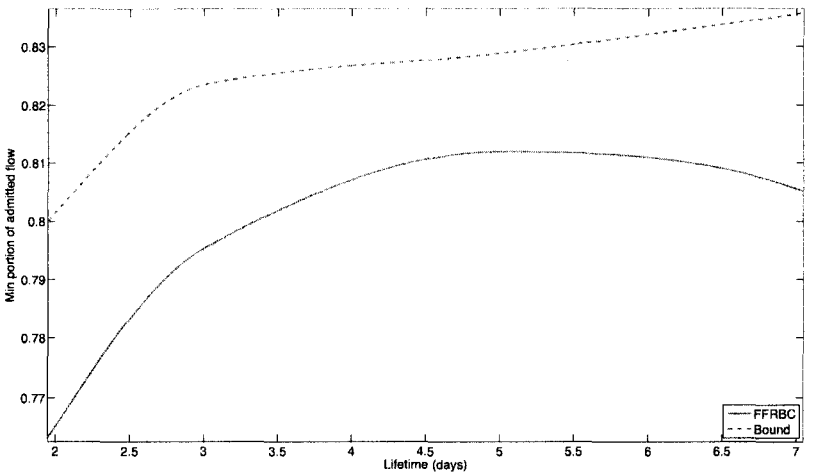

Figure 4.1: Minimum Portion of Admitted Bandwidth Flows vs. Lifetime

4.6 Simulation Model and Results

Using the proposed bandwidth control methodologies many experiments were conducted which study the performance of the algorithms. It is assumed that all nodes are solar powered and that the initial battery state is full prior to the deployment. For the bandwidth control, a number of random fixed bandwidth usage profiles were chosen. The number of bandwidth flows in the bandwidth usage profile is the same as the number of nodes in the network. Bandwidth flow rates were taken to be drawn from a normal distribution and the sources and destinations were chosen uniformly.

In the first set of experiments all bandwidth flows are assumed to have the same priority. The duration of each bandwidth flow is chosen to be the desired deployment duration, $\mathcal{T}_{\mathcal{L}}$. Some examples are shown that compare the bandwidth control bound to the FFRBC algorithm. The fairness of each case is plotted as the minimum portion of admitted bandwidth flow in all hours versus network lifetime. Figure 4.1 shows the average of 20 different random networks, each consisting of 10 nodes. As seen in Figure 4.1, the difference between the bound and FFRBC is not very large. This indicates that the proposed algorithm performs well.

Table 4.1 compares the network normal capacity for the optimal solution and the FFRBC algorithm versus network lifetime. The normal capacity is calculated as

$$\frac{\sum_{k\in\mathcal{K}}\sum_{b\in\mathcal{M}} A(b,k)\cdot M}{\mathcal{T}_{\mathcal{L}}}. \tag{4.12}$$

As seen in Table 4.1, the proposed causal algorithm has almost the same capacity as the

Lifetime	Bound	FFRBC
2	1.4879	1.4877
3	1.4886	1.4884
5	1.3965	1.3959
7	1.3941	1.3825

Table 4.1: Network Capacity for Optimum Bound vs Proposed FFRBC for Different Network Lifetimes

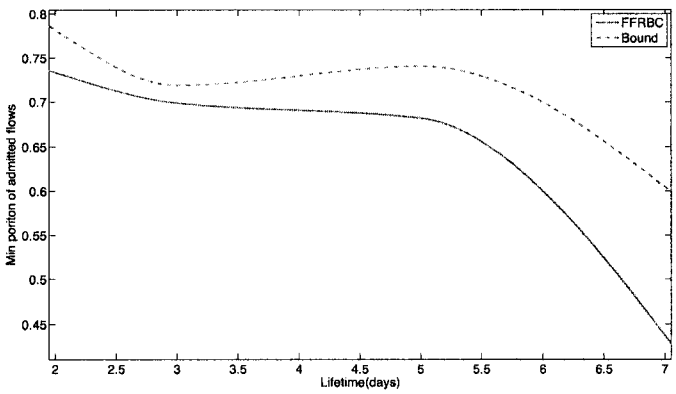

Figure 4.2: Minimum Portion of Admitted Bandwidth Flow vs. Lifetime with High Priority Bandwidth Flows

bound. This indicates that even if the proposed FFRBC algorithm is admitting a lower portion of the flows, it is doing that so rarely that it does not have a strong effect on the capacity. In the next set of results the FFRBC algorithm is compared to the bound given that half of the bandwidth flows are high priority flows (i.e., they have to be fully admitted). Figure 4.2 shows that the difference between the bound and the FFRBC algorithm is larger than the difference when there are no high priority bandwidth flows. This is because now the FFRBC algorithm has to fully admit the high priority bandwidth flows which consume a significant amount of energy at the beginning of the run, so FFRBC's actions become more conservative later. In addition, the minimum portion of admitted flow in both the bound and the proposed FFRBC is less than the case when there are no high priority bandwidth flows. This is because in this case both the bound and the FFRBC algorithm have to fully admit certain bandwidth flows which makes them less fair to the rest.

Lifetime	Bound	FFRBC
2	1.6048	1.6038
3	1.5711	1.5711
5	1.2937	1.2936
7	1.1556	1.1432

Table 4.2: Network Capacity for Bound vs FFRBC for Different Network Lifetimes with High Priority Bandwidth Flows

In the next table the total network capacity is compared for the optimal solution and the FFRBC algorithm versus network lifetime. Table 4.2 also indicates that even if FFRBC is admitting a lower portion of the flows, it is happening so rarely that it does not significantly affect the capacity.

In the second set of the experiments the bandwidth usage profile is assumed to be temporally variable (i.e. bandwidth flow rates and durations vary over time). The duration of each bandwidth flow is chosen from a uniform distribution between 1 and the desired deployment duration, $\mathcal{T}_{\mathcal{L}}$. Some examples are shown that compare the bound to the proposed FVRBC algorithm. The fairness of each case is plotted as the minimum portion of admitted bandwidth flow in all hours versus network lifetime. Figure 4.3 shows the average of 20 different random networks, each consisting of 10 nodes. As expected, the figure shows that the difference between the bound and FVRBC is greater than the difference between the bound and FFRBC. This is due to the fact that FVRBC deals with changes in the solar insolation data and the bandwidth usage profile.

In Figure 4.4 the network capacity for the bound and the FVRBC algorithm is compared. Note that the difference between both network capacities is very small, i.e., 2%. Again, this means that even if the FVRBC algorithm is admitting a lower portion of the flows, it is happening so rarely that it does not have a strong effect on the capacity. Moreover, the difference in network capacity for the variable bandwidth usage profile case is more than that in the fixed bandwidth usage profile case. This is due to the fact that the FVRBC algorithm has to adjust its calculations due to differences in solar insolation and bandwidth flows, which degrades the performance of the algorithm.

In the next set of results the FVRBC algorithm is compared to the bound given that half of the traffic flows are high priority bandwidth flows (i.e., as before, they must be fully admitted). Again, it can be seen in Figure 4.5 that the minimum portion of admitted flow for both the bound and the proposed FVRBC algorithm is smaller than that when there are no high priority bandwidth flows. This is because both the bound and the FVRBC algorithm have to fully admit certain bandwidth flows, which makes them less fair to the rest. Moreover, the difference between the bound and the FVRBC algorithm is larger than

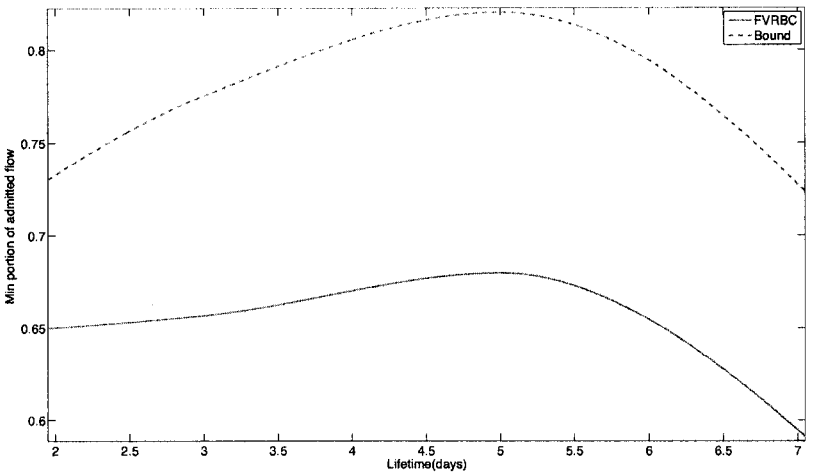

Figure 4.3: Minimum Portion of Admitted Bandwidth Flow vs. Lifetime with Variable BUP

in the former case. This is because the FVRBC algorithm has to fully admit the high priority bandwidth flows, which consume significant energy in the initial part of the deployment. As a result, FVRBC's actions get more conservative as time goes on.

In Figure 4.6 the network capacity is compared for the bound and the FVRBC algorithm when half of the traffic flows are high priority bandwidth flows. Again, as expected, the difference in the network capacity for the variable BUP case is more that that in the fixed BUP case. The difference between both network capacities is also about 2%.

4.7 Conclusions

In this chapter the fair bandwidth control problem has been considered for solar powered wireless mesh networks. A convex formulation for the problem was first introduced which gives upper bounds on the max/min fair network capacity. A methodology for doing the bandwidth control was then introduced, motivated by the optimization. Comparisons between the computed bounds and the proposed causal bandwidth control algorithms for different networks demonstrates the effectiveness of the proposed algorithms. The case where some of the bandwidth flows are high priority was also included, and it was found that the proposed causal bandwidth control algorithm performs well. However, the simulations showed that the proposed algorithms may have high computational complexity, which suggests that they must be run by a wired server with which the mesh nodes communicate.

In Chapter 5 the problem of traffic growth management in solar powered wireless mesh networks is addressed. A mathematical formulation for the problem is given to obtain a

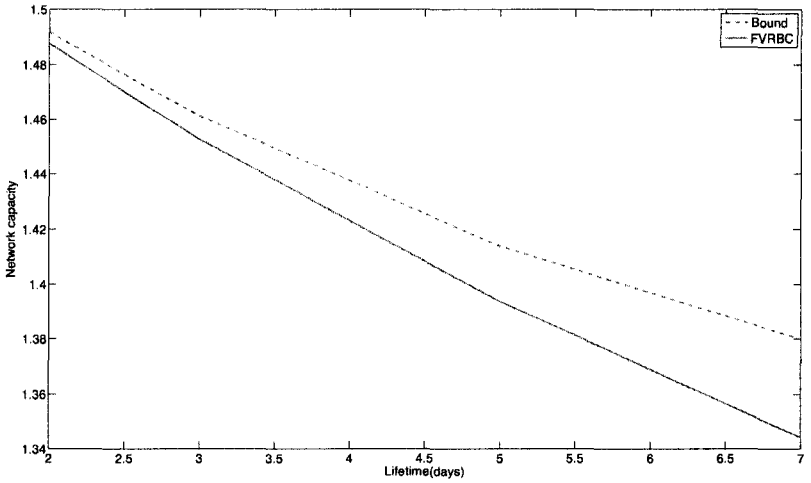

Figure 4.4: Network Capacity vs. Lifetime with Variable BUP

lower bound that can be used to study the proposed traffic growth management algorithms. A network deployed using the optimum allocations will experience outage since the optimum allocation uses knowledge of future solar insolation and thus two algorithms are proposed for determining practical resource upgrades. An optimization based algorithm is first introduced which is done by solving a local optimization problem using only past and current information. The results show that this algorithm successfully assigns new node resources, but does not perform well compared to the lower bound. This motivates the second approach based on genetic algorithms and the presented results show the significant cost savings that are possible using this approach.

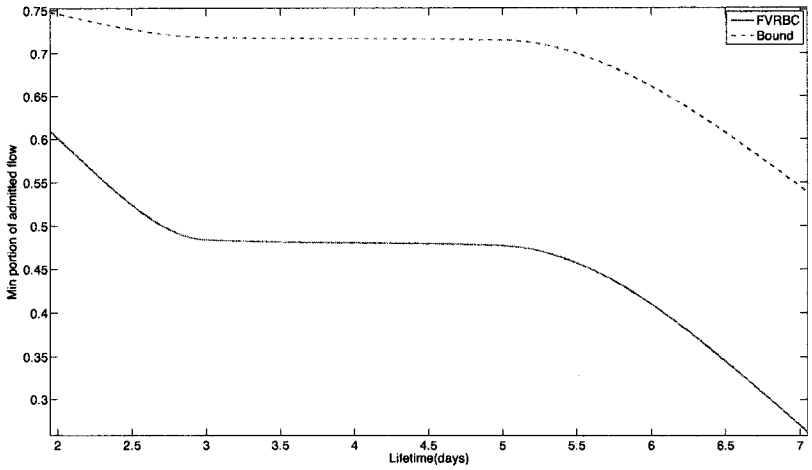

Figure 4.5: Minimum Portion of Admitted Flow vs. Lifetime with Variable BUP and High Priority Bandwidth Flows

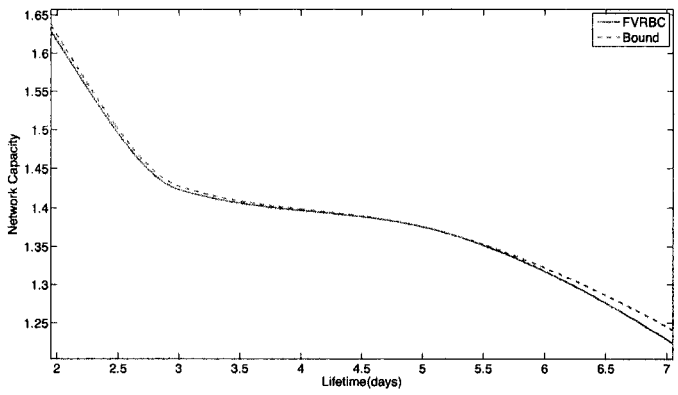

Figure 4.6: Network Capacity vs. Lifetime with Variable BUP and High Priority Bandwidth Flows

Chapter 5

Managing Traffic Growth in Solar Powered Wireless Mesh Networks

5.1 Introduction

As wireless mesh network (WMN) user traffic evolves over time, network resources must often be upgraded to accommodate increasing traffic demands. To address this, traditional network engineering typically includes the process of network capacity upgrading, which may involve adding new nodes and transmission links where they are needed. In the case of energy-sustainable networks, one must also consider the costs of updating the energy source and storage configurations of the nodes in order that the long-term sustainability of the network can be preserved.

In this chapter a methodology for addressing the problem of traffic evolution is proposed and studied in wireless networks that include sustainable energy mesh nodes. Resource assignment for these types of networks is normally done using a target load profile for the nodes, which is used to compute the power consumption workload for which the nodes are then configured. As discussed in previous chapters, the resource provisioning is usually done by subjecting the target network design to the traffic load profile using historical solar insolation data that is available for the desired deployment area. This is done over a time window, $\mathcal{T}_{\mathcal{L}}$, that is sufficient to ensure that the deployed network will operate without node outage for all time. Once the network is deployed however, its performance may become unreliable in cases when the traffic flows evolve beyond their original design. In these scenarios network resources must be upgraded to accommodate increasing traffic demands. For networks with solar powered mesh nodes, this problem includes updating not only link capacity but also increasing node energy resources. Since the resources needed by a node are dependent on the routing used in the network, this becomes a difficult problem to solve. Whenever the resource assignment changes, it alters the selection of routes, requiring a different resource assignment.

A performance bound on the network upgrade cost is formulated as a mixed integer linear program (MILP). This optimization is done over the target lifetime of the network and uses an optimal routing that assumes the knowledge of future solar insolation and traffic flows. This results in a lower bound on the network upgrade costs which can be used as a comparison with real provisioning algorithms. A technique based on a genetic algorithm approach is then introduced for determining low cost node resource upgrading. Results are given which show the value of the proposed algorithm.

5.2 Background

There has been a lot of previous work dealing with network engineering, however, to the best of our knowledge, it does not deal with WLAN mesh networks with sustainable energy. Methodologies often involve allocating resources so that future worse-case connection blocking rates can be met. In (Nayak and Sivarajan, 2002) a traffic growth model is introduced for optical networks with time-varying traffic arrivals. A nonlinear network dimensioning method is proposed based on a traffic growth model with cost minimization as the objective and route absorption probabilities as the constraints instead of blocking probability. In (Roy and Mukherjee, 2008) a new parameter is proposed for optical networks called network-cut exhaustion probability. This is defined as the probability that at least one light path request will be rejected during a specified time period due to a lack of capacity on that cut. A procedure was also proposed to calculate a lower bound on the network-cut exhaustion probability.

In (Bagula and Krzesinski, 2006) a network management scheme is presented where network engineering is used to complement traffic engineering in a multi-layer setting where a data network overlay is run over an optical network. A strategy is proposed based on a multi-constraint optimization model consisting of finding bandwidth-guaranteed IP tunnels subject to contention avoidance minimization and bandwidth usage maximization constraints. This is complemented by a traffic engineering model which uses a bandwidth trading mechanism to rapidly re-size and re-optimize the established tunnels under Quality of Service (QoS) mismatches between the traffic carried and the resources available. The performance of this hybrid strategy when routing, re-routing and re-sizing the tunnels was studied for a 23-node network.

In (Zhang, 2005) an upgrade problem is considered with budget constraints where arcs between nodes are updated to higher transmission rates. In (Campbell *et al.*, 2006) a series of problems is considered that involve finding the best q arcs in a network to upgrade with respect to different minimax network objectives. They also show that these problems are NP-hard on general graphs, but polynomially solvable on trees. Finally, three heuristics are compared for complete graphs based on the polynomial results. In (Lim *et al.*, 2005) a brute force technique is used to solve network engineering problems. The algorithm

finds the bottleneck link whose upgrade achieves a maximal improvement. The proposed methodology has a high computational cost and a heuristic is proposed that obtains the bottleneck link with a high probability.

Genetic algorithms have been used to manage traffic growth management in different types of networks, which includes air traffic networks, roadways, and wireless networks. In (Herabat and Tangphaisankun, 2005), genetic algorithms have been used to solve the problem of maintaining highways subject to budget and network system preservation constraints. The genetic algorithm chooses which parts of the highway should be widened or re-paved to sustain the traffic growth. The problem was modeled as a multi-objective optimization problem where the authors try to minimize the vehicle operating cost and maximize the overall road condition. In (Montana and Hussain, 2004) the authors use an approach based on genetic algorithms to reconfigure the topology and link capacities of an operational network. The networks are assumed to have both fixed links and reconfigurable links. The authors formulate the problem as an optimization that finds the optimal channel reconfiguration that will maximize the number of admitted flows and minimize the transmission delay and packet dropping rates. The results show that the proposed approach performs well but in its current form, it is too slow for online adoption. To make it fast enough for small and mid-sized networks, the authors suggest distributing the evaluations of the genetic algorithm across many machines.

5.3 Problem Formulation

In this section the resource update problem is formulated as a mixed integer linear programming (MILP) optimization. This formulation gives a bound that will be compared to practical algorithms later in the chapter.

Using definitions which are similar to those in Chapters 3 and 4, the problem is formulated as follows.

- The mesh network consists of N nodes modeled as a *directed graph* where each mesh node represents a vertex and two nodes can have an edge (i.e., a link) between them if they are within communication range. Each node is identified by an index in the set $\mathcal{N} = (1, 2, \ldots, N)$ and each edge is defined by an ordered pair (i, j) where $i, j \in \mathcal{N}$ are the transmitting and receiving nodes, respectively. The set of all edges is denoted by E. The network is assumed to be already deployed and the current battery capacity for Node i is referred to as $B_{old}(i)$, the current solar panel size is $P_{old}(i)$ and the current number of radios is $R_{old}(i)$. Traffic is relayed in a multi-hop fashion and a path from source to destination consists of one or more adjacent edges.

- Sample functions consisting of the new estimated bandwidth usage profile (BUP) and estimated solar insolation input trace are given for a contiguous deployment time period, $\mathcal{T}_{\mathcal{L}}$. The estimated usage profile consists of a multi-commodity bandwidth usage

matrix $\mathcal{M} = m_{sd}(k)$, where $m_{sd}(k) \geq 0$ indicates the aggregate bandwidth requirement from Node s to Node d during time period $((k-1)\Delta, k\Delta)$. The estimated solar insolation sample function consists of an input trace over the same time period whose values at Node i are given by $\mathcal{E}_{SIM}(i,k)$.

The deployment time period is given by $\mathcal{T}_{\mathcal{L}} = (k_{min}\Delta, k_{max}\Delta)$ where k runs over the set $\mathcal{K} = (k_{min}, k_{min}+1, \ldots, k_{max})$.

- The objective is to upgrade the current network by assigning $\mathcal{P}_{new}(i)$, $B_{new}(i)$ and $R_{new}(i)$ so that the total solar panel and battery resource provisioning update cost is minimized when Equation 3.1 is applied such that $B(i,k) > B_{outage}(i)$ for $k \in \mathcal{K}$ and $i \in \mathcal{N}$.

In order to generate practical traffic growth management algorithms, the sample function values must be provided to the system in a causal fashion so that future values are not known to the system as Equation 3.1 is evaluated. In order to investigate the quality of various traffic growth management mechanisms, in the next section a lower bound is derived on the network update cost. This bound is then compared with TGM and TGMGA introduced in Section 5.4.

5.3.1 Traffic Growth Management Optimization

Given the directed graph described above and the BUP, the objective is to minimize the update cost of the network. The update cost, $y(i)$, for each node, i, consists of the cost of the extra battery and solar panel resources, the cost of the extra radio links, and a fixed cost, $\gamma(i)$, that represents any fixed re-configuration costs for a given node. Therefore

$$y(i) = \gamma(i)(1-(1-z_P(i))(1-z_B(i))(1-z_R(i,j))) + C(i), \tag{5.1}$$

where $z_B(i), z_R(i,j), z_P(i)$ are binary variables that take the value of 1 if Node i requires a battery, panel or radio upgrade, and zero otherwise. $C(i)$ is defined as the total update cost at Node i given by $\rho_B \Delta B(i) + \rho_P \Delta P(i) + \rho_R \sum_{(i,j)\in E} \Delta R(i,j)$. In this expression, ρ_B, ρ_P and ρ_R are the unit battery, solar panel and radio costs. $\Delta B(i)$, $\Delta P(i)$ and $\Delta R(i,j)$ are defined as the difference between the new resource allocations and the current ones. $\Delta B(i)$ and $\Delta P(i)$ are taken to be real numbers and $\Delta R(i,j)$ is an integer. Moreover, $B_{new}(i)$ represents the new battery capacity needed and $P_{new}(i)$, and $R_{new}(i,j)$ represents the new panel size and the new number of radios needed at each Node i.

The optimization can be formulated with an objective that finds the minimum update cost subject to satisfying the routing and battery constraints, i.e., a Link (i,j) can only be assigned to a bandwidth flow when the energy levels at Nodes i and j are above $B_{outage}(i)$

for all k. The optimization problem can be written as follows.

$$minimize \sum_{i\in\mathcal{N}} y(i) + \lambda_1 \sum_{i\in\mathcal{N}}\sum_{k\in\mathcal{K}} L(i,k) + \lambda_2 \sum_{k\in\mathcal{K}}\sum_{i\in\mathcal{N}} s(i,k) \tag{5.2}$$

subject to the following constraints.

$$0 \leq f_{ij}(k) \leq R_{new}(i,j) \tag{5.3}$$

for all $(i,j) \in E, k \in \mathcal{K}$, and,

$$y(i) = \gamma(i)(1-(1-z_P(i))(1-z_B(i))(1-z_R(i,j))) + C(i) \tag{5.4}$$

$$z_B(i), z_P(i), z_R(i,j) \in \{0,1\} \tag{5.5}$$

$$\begin{aligned} \Delta B(i) &= B_{new}(i) - B_{old}(i), & (5.6)\\ \Delta P(i) &= P_{new}(i) - P_{old}(i), & (5.7)\\ \Delta R(i,j) &= R_{new}(i,j) - R_{old}(i,j), & (5.8) \end{aligned}$$

for all $i \in \mathcal{N}, (i,j) \in E$, and,

$$\begin{aligned} 0 \leq \Delta R(i,j) &\leq z_R(i,j) R_{max}(i,j) & (5.9)\\ 0 \leq \Delta B(i) &\leq z_B(i) B_{max}(i) & (5.10)\\ 0 \leq \Delta P(i) &\leq z_P(i) P_{max}(i) & (5.11) \end{aligned}$$

for all $i \in \mathcal{N}, (i,j) \in E$ and,

$$\sum_{(i,l)\in E} f_{il}(k) + \sum_{d\in\mathcal{N}} m_{id}(k) = \sum_{(h,i)\in E} f_{hi}(k) + \sum_{s\in\mathcal{N}} m_{si}(k) \tag{5.12}$$

for all $i \in \mathcal{N}, k \in \mathcal{K}$, and,

$$B_{outage}(i) \leq B(i,k) \leq B_{new}(i), \tag{5.13}$$

$$B(i,k) + s(i,k) = B(i,k-1) + P_{new}(i)\mathcal{E}(i,k) - L(i,k). \tag{5.14}$$

$$L(i,k) = (\sum_{(i,l)\in E} Rf_{il}(k) + \sum_{(i,l)\in E} T\alpha f_{il}(k) + \sum_{(h,i)\in E} Tf_{hi}(k) + \sum_{(h,i)\in E} R\alpha f_{hi}(k) + \sum_{(i,l)\in E} S(1 - x_{il}(k) - \alpha f_{il}(k)) + \sum_{(h,i)\in E} S(1 - x_{hi}(k) - \alpha f_{hi}(k)))\Delta \quad \forall i \in \mathcal{N}_s, k \in \mathcal{K}. \quad (5.15)$$

$f_{ij}(k)$ in Equation (5.3) , $y(i)$ in Equation (5.4) , and $z_B(i), z_R(i,j)$ and $z_P(i)$ in Equation (5.5) are the decision variables, where $y(i)$ is the update cost for Node i. Moreover, $f_{ij}(k)$ represents the traffic load on Link (i,j) at time k if $f_{ij}(k) \geq 0$ then link (i,j) is on the available paths at time instance k, otherwise $f_{ij}(k) = 0$ and $z_B(i), z_R(i,j), z_P(i)$ are the binary variables defined above in Equation (5.1). Constraint (5.3) is the link capacity constraint that ensures that the traffic load on each link is less than its total capacity. Constraints (5.6), (5.7), and (5.8) calculate the difference between the old and the new resources, where $\Delta B(i), \Delta P(i)$ and $\Delta R(i,j)$, represents the value of extra battery capacity or panel size and the new radios needed to sustain the new traffic flow at each Node i, respectively. Constraints (5.9), (5.10) and (5.11) ensure that $z_B(i), z_P(i)$ and $z_R(i,j)$ will have a value of 1 only when Node i is updated, i.e., when either $\Delta B(i), \Delta P(i)$ or $\Delta R(i,j)$ is greater than zero, respectively, where $B_{max}(i), P_{max}(i)$ and $R_{max}(i,j)$ are upper limits on the capacity of the battery or the size of panel and the number of radios for each Node i. This limit is imposed by physical or technical constraints. These constraints are needed to ensure that the fixed cost $\gamma(i)$ is only added to upgraded nodes. Constraint (5.12) ensures flow continuity by ensuring that the input flow at each node is equal to its output flow. Constraint (5.13) represents the upper and lower bounds on the energy levels at the battery for each Node i. They ensure that the energy level at each battery does not go below $B_{outage}(i)$ or above $B_{max}(i)$. Equation (5.14) is the battery energy flow recursion as described in Section 3.3. Constraint (5.15) is the energy consumed at each node where the first line represents the energy consumed for receiving a message and transmitting the ACKs and other associated reverse-link flows. The second line represents the energy consumed in transmitting a packet and receiving the ACKs and other associated reverse-link flows associated with that transmission. The third and fourth lines are the energy consumed in sleep mode.

The objective function in this problem minimizes the total update cost, the second term in the objective function minimizes the load on each node and is added to ensure that the optimizer will choose loop free routes. This term is added because our experiments have shown that the optimizer will generate loops in the routes if any nodes in a loop have extra energy. This does not affect the optimal solution because the optimizer will only expend energy at nodes that are not energy constrained. The third term in the objective function

minimizes the value of s as stated previously in Section 3.3.2 . λ_1 and λ_2 are control factors that are set so as to not interfere with the operation of the original objective.

All the above equations are linear except Equation (5.4). Binary linearization can be used to change the problem to a mixed integer linear programming (MILP) problem. Four new binary auxiliary variables for Node i will be defined, i.e., $\delta_{BR}(i), \delta_{PR}(i), \delta_{PB}(i), \delta_{PBR}(i)$, which represent one auxiliary variable for each product of the binary variables. Then the following constraints can be added

$$\delta_{BR}(i), \delta_{PR}(i), \delta_{PB}(i), \delta_{PBR}(i) \in \{0,1\} \tag{5.16}$$

$$\begin{aligned}
z_B(i) + z_P(i) - \delta_{PB}(i) &\leq 1, && (5.17)\\
-z_B(i) - z_P(i) + 2\delta_{PB}(i) &\leq 0, && (5.18)\\
z_B(i) + z_R(i) - \delta_{BR}(i) &\leq 1, && (5.19)\\
-z_B(i) - z_R(i) + 2\delta_{BR}(i) &\leq 0, && (5.20)\\
z_R(i) + z_P(i) - \delta_{PR}(i) &\leq 1, && (5.21)\\
-z_R(i) - z_P(i) + 2\delta_{PR}(i) &\leq 0, && (5.22)\\
z_B(i) + z_P(i) + z_R(i) - \delta_{PBR}(i) &\leq 2, && (5.23)\\
-z_B(i) - z_P(i) - z_R(i) + 3\delta_{PB}(i) &\leq 0, && (5.24)
\end{aligned}$$

$$\begin{aligned}
y(i) &= \gamma(i)(z_B(i) + z_P(i) + z_R(i) - \delta_{BR}(i) - \delta_{PB}(i)\\
&- \delta_{PR}(i) + \delta_{PBR}(i)) + C(i). && (5.25)
\end{aligned}$$

The above MILP uses a routing that assumes knowledge of future solar insolation. Since a real routing algorithm will not have this information, it will not necessarily choose optimal routes, and nodes may experience outage using this deployment update bound.

In the next section, traffic growth management algorithms are introduced that will use a practical routing algorithm. The first proposed algorithm uses the above optimization but on an hourly basis. The second uses a genetic algorithm approach.

5.4 Traffic Growth Management Algorithms

In this section two practical network resource provisioning update algorithms are proposed. In Section 5.5 they are compared to the bound derived in Section 5.3.1.

5.4.1 Traffic Growth Management Algorithm (TGM)

A straightforward technique is to run the optimization problem at each hourly system update epoch. In this way the algorithm does not use future information and will choose the optimal routing for that specific hour. Using the currently configured resources, the TGM Algorithm will run hourly. Since the new traffic matrix is different than the original, TGM will begin running into network outage and will add resources that will allow it to run until the end of the hour without outage. This process continues until the target lifetime of the network is reached. In Section 5.5 it is shown that this algorithm successfully assigns new node resources, but does not perform well compared to the lower bound. This motivates the use of a genetic algorithm (GA) proposed in the next section.

5.4.2 Traffic Growth Management using a Genetic Algorithm (TGMGA)

A genetic algorithm combined with energy aware routing is used to solve the traffic growth management problem. To emulate the routing algorithm that is used during the operation of the network, a genetic algorithm (GA) is used to choose a combination of battery capacities, panel sizes and radio configurations. If the network lives for the desired lifetime, $\mathcal{T}_{\mathcal{L}}$, then this combination is feasible, otherwise another combination is tested.

A chromosome of the proposed GA consists of sequences of positive real numbers representing the new battery capacity followed by the new solar panel size then the new number of radios for each node. The length of the chromosome is three times the number of nodes in the network. The choice of the population size is a very important factor in the GA. Small populations execute quickly but they may not explore the entire search space. By experimenting, a population size that is equal to twice the length of the chromosome was found to perform well for the problem. Uniform crossover is chosen, where the operator decides which parent will contribute each of the gene values in the offspring chromosomes. As mentioned above the chromosome represents the battery capacity, panel size and number of radios of each node, so using single point crossover will take one half of the new chromosome from a parent and the other half from the other parent which will not work well in our case.

Selection is a genetic operator that chooses a chromosome from the current generation's population for inclusion in the next generation's population. Before making it into the next generation's population, selected chromosomes may undergo crossover and/or mutation (depending upon the probability of crossover and mutation) in which case the offspring chromosome(s) are actually the ones that make it into the next generation's population. The right selection is critical in ensuring sufficient optimization progress on the one hand and in preserving genetic diversity to be able to escape from local optima on the other. Experiments have shown that the Remainder selection best suits this problem because it

Algorithm 3 GA/Routing Algorithm

```
for all k ≤ K_max do
    for all m ≤ M do
        Calculate the cost matrix.
        if k ≥ start(m) and k ≤ end(m) then
            Calculate the shortest path using Dijkstra's Algorithm.
            Update the load on each node.
        end if
    end for
end for
Update battery charges according to the load and solar insolation.
```

gives a high probability of diversity in the population.

Another parameter for the GA is the fitness function, $\mathcal{F}$. Our fitness function will accept the chosen set of $B_{new}(i), P_{new}(i), R_{new}(i,j)$ as an input and report the update cost of the network which is given by

$$\mathcal{F} = \begin{cases} \sum_{i \in \mathcal{N}} \gamma(i) C(i) & \Delta B(i) > 0 \\ & \Delta P(i) > 0 \\ & \sum_{(i,j) \in E} \Delta R(i,j) > 0 \\ 0 & otherwise \end{cases} \tag{5.26}$$

Here, $\Delta B(i)$, $\Delta P(i)$ and $\Delta R(i,j)$ are defined as in Equations (5.6), (5.7), and (5.8) respectively. The GA search space will be restricted as a constraint based on the lifetime of the network while using energy aware routing.

The causal energy aware routing algorithm uses the Dijkstra shortest path algorithm, using the same cost function as the one proposed in Zeng *et al.* (2009), i.e.,

$$\frac{1}{\zeta^{B(i,k)/B_{max}(i)} \cdot \mathcal{E}(i,k)}, \tag{5.27}$$

where ζ is a large constant. The cost of a route is the number of links crossed by the route. This process is summarized in Algorithm 3. At every hour, k, the shortest path for the traffic flow, m , running at this hour (i.e., the start time of traffic flow m is before the current hour and the end time for the same traffic flow is after the current hour) is calculated according to the cost matrix. After calculating the path, the load on every node is updated according to the traffic flows passing through it as indicated in Equation (5.15). Then the battery charge is updated at each node according to Equation (5.14).

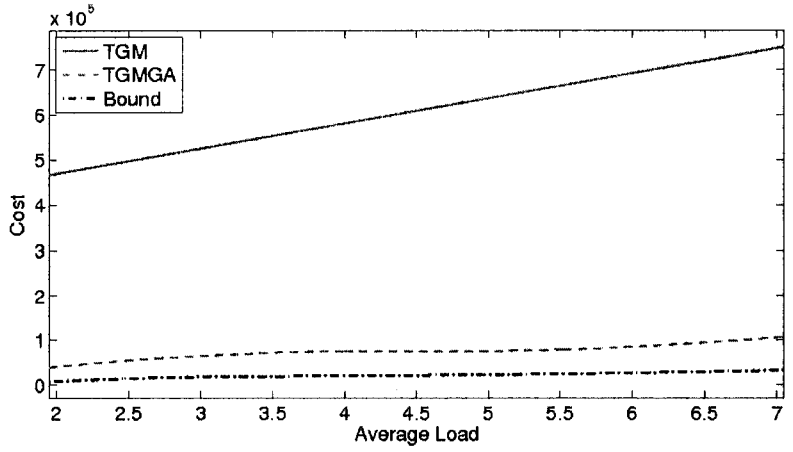

Figure 5.1: Total Update Cost versus Average Load for Random Networks

5.5 Simulation Model and Results

Using the proposed methodology many experiments have been done which show the reductions in network update cost that are possible. First, all nodes are assumed to be solar powered and that the initial battery state is full prior to the deployment. For the initial resource provisioning, a number of random fixed traffic matrices were chosen. Each source introduces a maximum traffic flow which is used as the traffic profile. This traffic flow rate is chosen randomly from a uniform distribution between zero and one. In all of the experiments, the traffic flows are assumed to be temporally variable, as would typically be the case in practice. The duration of each traffic flow is also chosen randomly from a uniform distribution between 1 and $\mathcal{T}_{\mathcal{L}}$. After the initial resource assignment is done, the flow matrices are scaled by a factor that represents the average load in the network.

In the first set of experiments the network update cost is compared for the bound, TGM and TGMGA versus different average loads in 20 node random networks. Figure 5.1 shows that TGMGA achieves almost 80% savings when compared to TGM. It can also be noted that the increase in the network cost is linear with the increase in the average load. Moreover, the figure shows that as the average load increases the update cost savings that are gained from TGMGA increase. As the network becomes overloaded TGMGA benefits from the energy aware routing while TGM keeps adding resources at each time epoch to accommodate the extra load. TGM doesn't perform as well as TGMGA because TGM chooses the minimum update cost for every time epoch. This greedy behavior leads to an over provisioning of the network. On the other hand, TGMGA finds the minimum upgrade cost for the entire network lifetime.

In Table 5.1 the network update cost for the bound, TGM, and TGMGA versus different

Average Load	Grid Networks			Tree Networks		
	Opt	TGM	TGMGA	Opt	TGM	TGMGA
2	1.02	49.1	8.5	7.7	167.9	44.0
3	1.7	53.8	9.9	12.2	198.9	104.7
4	2.4	58.5	10.6	16.7	229.9	75.7
5	3.3	63.3	11.5	21.2	260.9	60.7
6	4.4	68.0	13.0	25.7	291.9	69.4
7	5.6	72.7	14.2	30.2	332.3	75.5

Table 5.1: Cost vs. Network Type for Different Average Loading ($\times 10^3$)

average loads in 3×3 mesh networks and 15 node tree networks is compared. Again TGMGA achieves about 80% savings when compared to TGM. Moreover, the increase in cost is linear with the increase in the average load for both network topologies. It can also be noted that as in the random network case, in tree networks the cost savings gained from TGMGA increases as the average load increases. This is not true for grid networks because there are many shortest path routes, and as the load increases, all routing algorithms will need to increase the resources.

In Figure 5.2 the competitive ratio of the networks that were designed using the optimization is calculated. The competitive ratio (CR) is defined as the ratio between the actual lifetime of the network and the design lifetime using the same traffic matrix. It is shown that the network will not live for the desired lifetime because the optimization uses optimal routing which is not the same routing as the one used during network deployment. Figure 5.2 shows that for random networks the CR decreases slowly with the increase in the average load. However, in the grid case the CR is found to be almost constant except when there is a sharp decrease. This is explained by the fact that in a grid there are more paths for the routing to chose from than in the random networks case where the number of paths between sources and destinations is reduced. This helps the network to live longer by using different paths but as the average load increases the network becomes more sensitive to the resource assignment, and the lifetime decreases. In addition it can be noted that the CR for tree networks is the same for all average loads. Moreover, random networks have the lowest CR. The results also show that random networks have the lowest cost. This suggested that random networks are more sensitive to the resource assignment than the other topologies that are considered.

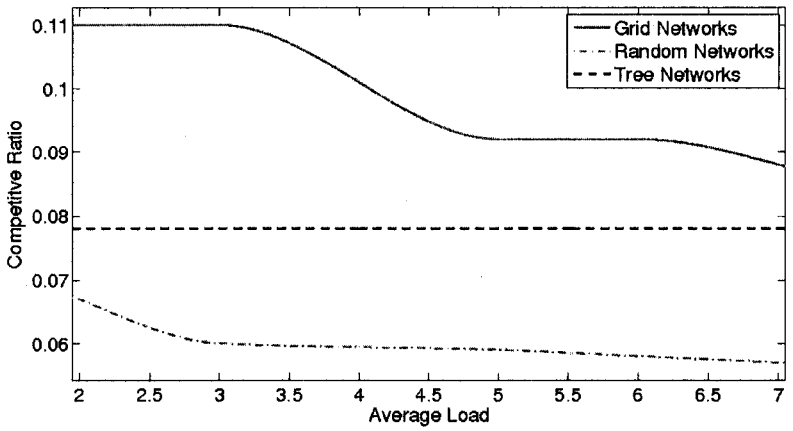

Figure 5.2: Competitive ratio versus Average Load for Different Network Topologies

5.6 Conclusions

In this chapter, the traffic growth management problem has been considered in wireless mesh networks that include solar powered mesh nodes. The update problem has been formulated as a mixed integer linear program which is used to find lower bounds on the update costs. A network deployed using the optimum allocations will experience outage and thus two algorithms for determining practical resource upgrades have been proposed. One is based on a local optimization and the other uses a genetic algorithm approach. The proposed algorithms may have scalability issues for large networks but since the focus is on wireless mesh infrastructure where the maximum hop counts rarely exceed 3 or 4, scalability is less of a concern. Also, this is an off-line design problem which can be done long before the actual upgrading occurs. Although the worst case complexity is exponential, branch and bound solutions typical do much better and this is what was experienced in the experiments. The results show that the genetic algorithm obtains the best results and performs favorably compared with the lower bound.

The thesis is concluded in the next chapter.

Chapter 6

Conclusions and Future Work

The recent interest in wireless mesh networking has resulted in the need to deploy wireless mesh APs in inaccessible places where the electrical power grid is not available. Solar powered wireless mesh nodes are increasingly used in these designs.

In this thesis resource management issues for solar powered wireless mesh networks were considered. First, the resource provisioning problem was studied. The objective for this type of provisioning is to find an assignment which ensures outage-free operation based on historical solar insolation traces and an input bandwidth load profile for the network. The problem was formulated as a linear programming optimization which found lower bounds that were used to verify the efficiency of the proposed schemes. Based on conventional single system photo-voltaic provisioning approaches, a flow-based provisioning procedure (SPRP) was first introduced. This method is based on deriving temporal shortest path routes, and then simulating each node independently using its energy flow equation and a power dissipation model. The large cost differences between the bound and SPRP motivated the development of a new methodology based on energy aware routing (EARP). EARP uses genetic algorithms to incorporate energy aware routing with resource provisioning. Results based on extensive simulations showed the large savings (around 60%) that can be achieved using EARP. They also showed that as the route diversity in the network decreases, more savings can be obtained from an energy aware resource provisioning. Moreover, it has been shown that the network cost savings in summer deployments are higher than in winter. This is because in summer there is much higher solar energy and energy aware routing more effectively uses routes that can harvest this energy. From a network resiliency viewpoint, it can be seen that the competitive ratio of EARP is lower than that of SPRP. This trend decreases when the network becomes heavily overloaded in the cases that were considered. In conclusion, significant cost savings can be achieved by using energy aware routing when provisioning the network compared to using SPRP. All these savings are increased substantially in hybrid networks when a mixture of solar and continuously powered nodes were considered

The resource provisioning output from EARP doesn't guarantee that the network will be outage-free in the future, since the provisioning was done using random sample functions of the BUP and the solar insolation processes. For this reason a fair bandwidth control mechanism was proposed. The proposed mechanism ensures that the bandwidth deficit resulting from the control action will be applied in a manner that is both temporally and spatially fair. The problem was formulated as a convex optimization using a fairness utility function. Based on knowledge of future solar insolation and the BUP, the optimization gives a max/min fair upper bound. Using an iterative local optimization mechanism, two causal bandwidth control mechanisms were then presented, Fair Fixed Rate Bandwidth Control (FFRBC) and Fair Variable Rate Bandwidth Control (FVRBC). FFRBC assumes that the BUP is fixed over the network lifetime while FVRBC assumes that the BUP is temporally variable. Results have shown that both algorithms perform well when compared to the bound. The case when the BUP had high priority bandwidth flows that had to be fully admitted was also considered. Results show that FFRBC performs better than FVRBC which is expected since FVRBC makes its decisions based on estimated bandwidth flows, not the actual flows as in FFRBC. Using the minimum portion of admitted flows as a fairness measure, the results show that the proposed algorithms have lower fairness than the bound. However, it has been shown that the maximum capacity difference between the proposed algorithms and the bound is 2%. This ensures that even if the proposed algorithms are admitting a lower portion of flow than the bound, they are doing it very rarely, so that it doesn't affect the network capacity.

As the user traffic evolves over time, the bandwidth deficit resulting from the bandwidth control algorithm may be unacceptable. To solve this problem, network resources must be upgraded to accommodate the increasing traffic demand. In Chapter 5, a methodology for addressing the problem of traffic evolution was proposed and studied. A performance bound on the network upgrade cost was formulated as a mixed integer linear program (MILP) optimization. This optimization was done over the target lifetime of the network and used an optimal routing that assumed knowledge of future solar insolation and the BUP. This resulted in a lower bound on the network upgrade cost that was used as a comparison with real provisioning algorithms. Two traffic growth management algorithms were introduced, Traffic growth management (TGM) and traffic growth management using GA (TGMGA). TGM is based on iterative local optimization, where the algorithm solves an optimization problem at every time epoch using only current and historical data. Results show that TGM doesn't perform well when compared to the bound, and this motivated the development of a new algorithm based on a genetic algorithm (TGMGA). Results show that TGMGA preforms very well when compared to the bound for different network topologies. It has also been shown that random networks are more sensitive to the resource assignment than the other topologies that were considered.

The work in this thesis can be extended in the future by considering other types of renewable energy sources. Moreover, the Chapter 4 results have shown that the proposed

algorithms are computationally complex so new distributed algorithms may be proposed to solve this issue. The traffic growth management problem may be extended to include nodes that are continuously powered. Adding continuously powered nodes to the traffic management problem creates some interesting extensions. One of these is to consider the problem when the node types can be changed (solar powered could be changed to continuously powered nodes). Finally, the work in this thesis assumes a constant transmission power for all nodes, and an interesting extension would be to examine the effect of node power control on the resource provisioning.

Bibliography

Ahn, C. W. and Ramakrishna, R. (2002). A Genetic Algorithm for Shortest Path Routing Problem and the Sizing of Populations. *IEEE Transactions on Evolutionary Computing*, **6**(6), 566–579.

Akyildiz, I., Wang, X., and Wang, W. (2005). Wireless Mesh Networks: A Survey. *Computer Networks and ISDN Systems*, **47**, 445–487.

Badawy, G., Sayegh, A., and Todd, T. (2008). Energy Aware Provisioning in Solar Powered WLAN Mesh Networks. *Proceedings of 17th International Conference on Computer Communications and Networks (ICCCN'08)*, pages 1–6.

Bagula, A. and Krzesinski, A. (2006). Traffic and Network Engineering in Emerging Generation IP Networks: A Bandwidth on Demand Model. *Proceedings of 1st IEEE International Workshop on Bandwidth on Demand*, pages 36–43.

Borowy, B. and Salameh, Z. (1996). Methodology for Optimally Sizing the Combination of a Battery Bank and PV Array in a Wind/PV Hybrid System. *IEEE Transactions on Energy Conversion*, **11**(2), 367–375.

BOSCO (2007). http://www.bosco-uganda.org/.

Boudec, J. (2008). Rate Adaptation, Congestion Control and Fairness: A Tutorial. *Ecole Polytechnique Federale de Lausanne (EPFL), Technical Report*, pages 8–16.

Camp, J. and Knightly, E. (2008). The IEEE 802.11s Extended Service Set Mesh Networking Standard. *IEEE Communications Magazine*, **46**, 120–126.

Campbell, A., Lowe, T., and Zhang, L. (2006). Upgrading Arcs to Minimize the Maximum Travel Time in a Network. *Networks*, **47**, 72–80.

Chang, J. and Tassiulas, L. (2004). Maximum Life Time Routing in Wireless Sensor Networks. *IEEE/ACM Transactions on Networking*, **12**, 609 – 619.

Chedid, R. and Rahman, S. (1997). Unit Sizing and Control of Wind-solar Power Systems. *IEEE Transactions on Energy Conversion*, **12**(1), 79–85.

Chen, S. and Zhang, Z. (2006). Localized Algorithm for Aggregate Fairness in Wireless Sensor Networks. *Proceedings of 12th Annual International Conference on Mobile Computing and Networking*, pages 274 – 285.

Choi, M., Jin, S., and Choi, S. (2007). Power Saving for Multi-Radio Relay Nodes in IEEE 802.11 Infrastructure Networks. In *Proceedings of IEEE Asia Pacific Wireless Communications Symposium (APWCS) 2007.*

Ergen, M. (2002). IEEE 802.11 Tutorial. University of California Berkeley,Technical Report.

Farbod, A. and Todd, T. (2004). SolarMESH Resource Allocation. *Internal Report. McMaster University*, pages 1–4.

Farbod, A. and Todd, T. (2006). Resource Allocation and Outage Control for Solar-Powered WLAN Mesh Networks. *IEEE Transactions on Mobile Computing*, **6**, 960–970.

Green WiFi (2007). http://www.green-wifi.org/.

Herabat, P. and Tangphaisankun, A. (2005). Multi-Objective Optimization Model using Constraint-Based Genetic Algorithms for Thailand Pavement Management. *Journal of the Eastern Asia Society for Transportation Studies,*, **6**, 1137 – 1152.

Hsieh, H. and Sivakumar, R. (2001). Improving Fairness and Throughput in Multi-Hop Wireless Networks. *Proceedings of IEEE International Conference on Networks (ICN)*, pages 569–578.

Huang, H. and Peng, Y. (2008). Throughput Maximization with Traffic Profile in Wireless Mesh Network. *Proceedings of the 14th Annual International Conference on Computing and Combinatorics*, pages 531–540.

IEEE 802.11e (2005). http://en.wikipedia.org/wiki/IEEE802.11e2005.

IEEE802.11 (2008). IEEE 802.11 Standard Group Web Site. http://www.ieee802.org/11/.

IEEE802.15 (2008). IEEE 802.15 Standard Group Web Site. http://www.ieee802.org/15/.

IEEE802.16 (2008). IEEE 802.16 Standard Group Web Site. http://www.ieee802.org/16/.

Inveneo (2007). http://www.inveneo.org/.

IR Data Corporation (2007). http://www.irdatacorp.com/.

Johansson, M. and Xiao, L. (2004). Scheduling, Routing and Power Allocation for Fairness in Wireless Networks. *IEEE Vehicular Technology Conference*, pages 1355 – 1360.

Kamali, G., Moradi, I., and Khalili, A. (2006). Estimating Solar Radiation on Tilted Surfaces with Various Orientations: A Case Study in Karaj (Iran). *Theoretical and Applied Climatology*, **84**, 235–241.

Kasten, A. (1996). A New Table and Approximate Formulas for Relative Optical Air Mass. *Arch. Metereol Geophys Bioklimatol Ser B*, **14**, 206–223.

Klein, S. (1977). Calculation of Monthly Average Insolation on Tilted Surfaces. *Solar Energy*, **19**, 325–329.

Ko, K., Tang, K., Chan, C., Man, K., and Kwong, S. (1997). Using Genetic Algorithms to Design Mesh Networks. *IEEE Computer*, **30**(8), 56–61.

Krishnamurthy, L. (2004). Making Radios More Like Human Ears: Alternative MAC Techniques and Innovative Platforms to Enable Large-Scale Meshes. *Microsoft Mesh Networking Summit.*

Li, L., Halpern, J., Bahl, P., Wang, Y.-M., and Wattenhofer, R. (2002). A Cone-Based Distributed Topology-Control Algorithm for Wireless Multi-Hop Networks. *IEEE/ACM Transactions on Networking*, **13**, 147–159.

Li, Y., Todd, T., and Zhao, D. (2005). Access Point Power Saving in Solar/Battery Powered IEEE 802.11 ESS Mesh Networks. *Proceedings of the 2nd Int'l Conf. on Quality of Service in Heterogeneous Wired/Wireless Networks*, pages 49–54.

Li, Y., Harms, J., and Holte, R. (2006). Traffic-Oblivious Energy-Aware Routing for Multihop Wireless Networks. *Proceedings of IEEE INFOCOM*, pages 1–12.

Lim, K., Soh, S., and Rai, S. (2005). Computer Communication Network Upgrade for Optimal Capacity Related Reliability. *Proceedings of Asia-Pacific Conference on Communications*, pages 1102–1107.

Lin, L., Shroff, N., and Srikant, R. (2005). Asymptotically Optimal Power-Aware Routing for Multihop Wireless Networks with Renewable Energy Sources. *Proceedings of the 24th Annual Joint Conference of the IEEE Computer and Communications Societies*, **2**, 1262–1272.

Lopez, R. and Agustin, J. (2005). Design And Control Strategies Of PV-Diesel Systems Using Genetic Algorithms. *Solar Energy*, **79**, 33–46.

Lumin Innovation Products Inc (2007). http://www.luminip.com/.

Maghraby, H., Shwehdi, M., and Al-Bassam, G. (2002). Probabilistic Assessment of Photovoltaic (PV) Generation System. *IEEE Transactions on Power Systems*, **17**(1), 205–208.

Mangold, S., Choi, S., May, P., Klein, O., Hiertz, G., and Stibor, L. (2002). IEEE 802.11e Wireless LAN for Quality of Service. In *Proceedings of European Wireless (EW'02)*, pages 32–39.

Marczyk, A. (2004). Genetic Algorithms and Evolutionary Computation. http://www.talkorigins.org/faqs/genalg/genalg.html.

Meraki (2007). http://www.meraki.com/.

Montana, D. and Hussain, T. (2004). Adaptive Reconfiguration of Data Networks Using Genetic Algorithms. *Applied Soft Computing,*, **4**, 433–444.

Narvarte, L. and Lorenzo, E. (2000). On the Usefulness of Stand-Alone PV Sizing Methods. *Progress in Photovoltaics: Research and Applications*, **8**, 391–409.

Nayak, T. and Sivarajan, K. (2002). Dimensioning Optical Networks Under Traffic Growth Models. *Proceedings of IEEE International Conference on Communications. (ICC)*, pages 2822–2826.

Neely, M., Modiano, E., and Li, C. (2008). Fairness and Optimal Stochastic Control for Heterogeneous Network. *IEEE/ACM Transactions on Networking*, **16**, 396–409.

Ni, Q., Romdhani, L., and Turletti, T. (2004). A Survey of QoS Enhancements for IEEE 802.11 Wireless LAN. *Wiley Journal of Wireless Communication and Mobile Computing (JWCMC)*, **4**, 547–566.

Park WiFi Project (2007). http://www.parkwifi.com/.

Perez, R. and Stewart, R. (1986). Solar Irradiance Conversion Models. *Solar Cells*, **18**, 213–222.

Perez, R., Ineichen, P., Seals, R., Michalsky, J., and Stewart, R. (1990). Modeling Daylight Availability and Irradiance Components from Direct and Global Irradiance. *Solar Energy*, **44**, 271–289.

Perez-Costa, X., D.Camps-Mur, and Vidal, A. (2007). On the Distributed Power Saving Mechanisms of Wireless LANs 802.11e U-APSD vs 802.11 Power Save Mode. *Elsevier Computer Networks Journal (CN)*, **51**, 2326–2344.

Rawlins, G. (1991). *Foundations of Genetic Algorithms*. Morgan Kaufmann Publishers.

Retvari, G., Biro, J., and Cinkler, T. (2007). Routing-Independent Fairness in Capacitated Network. *Proceedings of IEEE International Communications Conference (ICC)*, pages 6344–6349.

Riedl, A. (1998). A Versatile Genetic Algorithm for Network Planning. *Proceedings of the Open European Summer School on Network Management and Operation (EUNICE'98)*, pages 97–103.

Roy, R. and Mukherjee, B. (2008). Managing Traffic Growth in Telecom Mesh Networks (Invited Paper). *Proceedings of 17th International Conference on Computer Communications and Networks. (ICCCN)*, pages 1–6.

Saengthong, S. and Premrudeepreechacharn, S. (2000). A Simple Method in Sizing Related to the Reliability Supply of Small Stand-Alone Photovoltaic Systems. *Conference Record of the Twenty-Eighth IEEE Photovoltaic Specialists Conference*, pages 1630–1633.

Safie, F. (1989). Probabilistic Modeling of Solar Power Systems. *Proceedings of Reliability and Maintainability Symposium*, pages 425–430.

Sayegh, A. (2008). *Resource Allocation in Energy Sustainable Wireless Mesh Networks*. Ph.D. thesis, McMaster University, Hamilton, Ontario, Canada.

Sayegh, A. and Todd, T. (2007). Energy Management in Solar Powered WLAN Mesh Nodes Using Online Meteorological Data. In *Proceedings of IEEE International Communications Conference*, pages 3811–3816.

Sayegh, A., Todd, T., and Smadi, M. (2008). Resource Allocation and Cost in Hybrid Solar/Wind Powered WLAN Mesh Nodes. *Wireless Mesh Networks: Architectures and Protocols.*

Shagdar, O. and Zhang, B. (2005). Improving Per-Flow Fairness in Wireless Ad Hoc Network. *Proceedings of IEEE Wireless Communications & Networking Conference (WCNC)*, pages 2149–2154.

Shahirinia, A., Tafreshi, S., Gastaj, A., and Moghaddomjoo, A. (2005). Optimal Sizing Of Hybrid Power System Using Genetic Algorithm. *Proceedings of International Conference on Future Power Systems*, page 6.

Sirikonda, S. (2007). Multihop Routing Optimization In Communication Networks Using Genetic Algorithms. *M.S. Report, The University of Kansas, Lawrence, KS, USA.*

Soga, K., Akasaka, H., and Nimiya, H. (1999). A Comparison of Methods to Estimate Hourly Total Irradiation on Tilted Surfaces from Hourly Global Irradiation on a Horizontal Surface. *Proceedings of International Builfing Performace Simulation Association (IBPSA) Conference.*

Todd, T., Sayegh, A., Smadi, M., and Zhao, D. (2008). The Need for Access Point Power Saving in Solar Powered WLAN Mesh Networks. *IEEE Network Magazine*, **22**, 4–10.

Wong, T., Wong, H., and Drossopoulou, S. (1996). Applications of Genetic Algorithms. http://www.doc.ic.ac.uk/ nd/surprise_96/journal/vol4/tcw2/report.html.

Xu, D., Kang, L., Chang, L., and Cao, B. (2005). Optimal Sizing of Standalone Hybrid Wind/PV Power Systems using Genetic Algorithms. *Proceedings of Canadian Conference on Electrical and Computer Engineering*, pages 1722–1725.

Zeng, K., Ren, K., and Lou, W. (2009). Energy-Aware Geographic Routing In Lossy Wireless Sensor Networks With Environmental Energy Supply. *ACM Wireless Networks (WINET)*, **15**, 39–51.

Zhang, F., Todd, T., Zhao, D., and Kezys, V. (2004). Power Saving Access Points for IEEE 802.11 Wireless Network Infrastructure. *IEEE Wireless Communications and Networking Conference (WCNC)*, pages 195– 200.

Zhang, L. (2005). Upgrading Arc Problem with Budget Constraint. *Proceedings of the 43rd ACM annual Southeast regional conference*, pages 150 – 152.

Zhu, J., Hung, K., Bensaou, B., and Nait-Abdesselam, F. (2006). Tradeoff Between Network Lifetime and Fair Rate Allocation in Wireless Sensor Networks with Multi-Path Routing. *Proceedings of ACM International Conference on Modeling, Analysis and Simulation of Wireless and Mobile Systems (MSWiM)*, pages 301–308.